FEDERAL RESERVE BANK OF SAN FRANCISCO

WORKING PAPER SERIES

Pricing Deflation Risk with U.S. Treasury Yields

Jens H.E. Christensen
Federal Reserve Bank of San Francisco

Jose A. Lopez
Federal Reserve Bank of San Francisco

Glenn D. Rudebusch
Federal Reserve Bank of San Francisco

July 2014

Working Paper 2012-07
http://www.frbsf.org/publications/economics/papers/2012/wp12-07bk.pdf

Pricing Deflation Risk with U.S. Treasury Yields

Jens H. E. Christensen

Jose A. Lopez

and

Glenn D. Rudebusch

Federal Reserve Bank of San Francisco

Abstract

We use an arbitrage-free term structure model with spanned stochastic volatility to determine the value of the deflation protection option embedded in Treasury inflation-protected securities (TIPS). The model accurately prices the deflation protection option prior to the financial crisis when its value was near zero; at the peak of the crisis in late 2008 when deflationary concerns spiked sharply; and in the post-crisis period. During 2009, the average value of this option at the five-year maturity was 41 basis points on a par-yield basis. The option value is shown to be closely linked to overall market uncertainty as measured by the VIX, especially during and after the 2008 financial crisis.

JEL Classification: E43, E47, G12, G13.

Keywords: TIPS, deflation risk, term structure modeling.

We thank participants at the 2012 AFA meetings, FRB Chicago Day Ahead Conference, and the 15th Annual Conference of the Swiss Society for Financial Market Research for helpful comments, especially our discussants Kenneth Singleton, Andrea Ajello, and Rainer Baule. We also thank participants at the FDIC's 21st Derivatives Securities & Risk Management Conference, the Second Humboldt-Copenhagen Conference, and the Fourth Annual SoFiE Conference for helpful comments on previous drafts of the paper. Finally, we thank James Gillan and Justin Weidner for excellent research assistance. The views in this paper are solely the responsibility of the authors and should not be interpreted as reflecting the views of the Federal Reserve Bank of San Francisco or the Board of Governors of the Federal Reserve System.

This version: July 18, 2014.

1 Introduction

The U.S. Treasury first issued inflation-indexed bonds, which are now commonly known as Treasury inflation-protected securities (TIPS), in 1997. TIPS provide inflation protection since their coupons and principal payments are indexed to the headline Consumer Price Index (CPI) produced by the Bureau of Labor Statistics.[1] In addition, TIPS provide some protection against price deflation since their principal payments are not permitted to decrease below their original par value.

This deflation protection option has received limited attention in the literature, most likely since it has not been of much value in the U.S. inflationary environment since 1997. However, the sharp drops in price indexes during the financial crisis that started in the fall of 2008 increased deflationary concerns markedly, thus providing further motivation for examining the value of this protection. Two recent papers have used different arbitrage-free term structure models to assess the values of these deflation protection options.

Grishchenko et al. (2013) use a Gaussian affine model whose two factors are nominal Treasury rates and the inflation rate observed at the monthly frequency. They found that the option value is close to zero for most months, except for the deflationary periods observed in 2003-2004 and in 2008-2009. They calculate the maximum observed option value in December 2008 to be roughly 45 basis points of TIPS par value. On a par-yield basis, assuming a duration of four years for a five-year TIPS, this translates into a yield spread of approximately 10 basis points.

Christensen et al. (2012) use a "yields-only" approach based on a Gaussian affine model developed by Christensen et al. (2010, henceforth CLR) to value these deflation protection options. That model uses four factors to capture the joint dynamics of the nominal and real Treasury yield curves. The first three factors can be characterized as the level, slope, and curvature of the nominal yield curve, while the fourth factor can be characterized as the level of the real yield curve. The authors find that the option value, measured as a par-yield spread between two TIPS of similar remaining maturity but of differing vintages, reached a maximum of almost 80 basis points in December 2008 for TIPS maturing in 2013. This option value series is labeled the "CV model" in Figure 1. While the model-implied option value is highly correlated with the observed TIPS spread chosen as a proxy for the deflation protection option value, the implied values are mainly lower than the observed values. The authors suggest that this shortcoming could be addressed by incorporating stochastic volatility into the model in the hope of better characterizing the lower tail of the model-implied distribution of inflation outcomes.

[1]The actual indexation has a lag structure since the Bureau of Labor Statistics publishes price index values with a one-month lag; that is, the index for a given month is released in the middle of the subsequent month. The reference CPI is thus set to be a weighted average of the CPI for the second and third months prior to the month of maturity. See Gürkaynak et al. (2010) for a detailed discussion as well as Campbell et al. (2009) for an overview of inflation-indexed bonds.

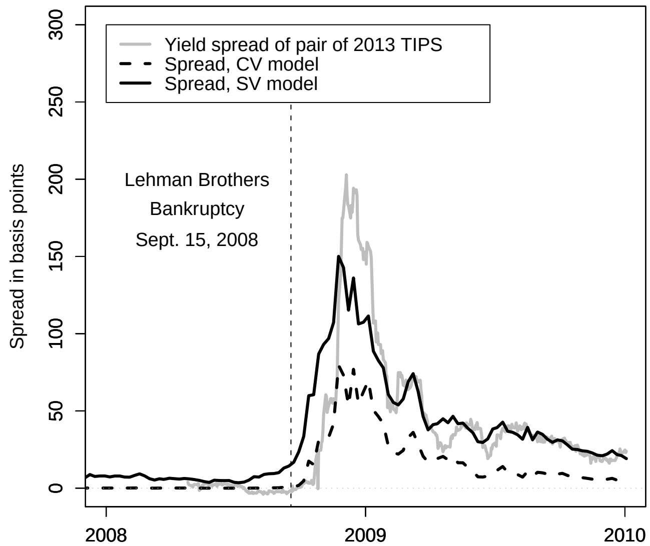

Figure 1: **Yield Spread between a Pair of 2013 TIPS as a Proxy for the Value of the Embedded Deflation Protection Option.**
Illustration of the spread in the yield-to-maturity as reported by Bloomberg between the seasoned ten-year TIPS that matures on July 15, 2013, and the newly issued five-year TIPS that matures on April 15, 2013. Included are the model-implied five-year par-coupon yield spreads from the CV model and the SV model introduced in this paper.

In this paper, we modify the latter model of nominal and real Treasury yields to incorporate spanned stochastic volatility.[2] In particular, the volatility dynamics are specified to be driven by the nominal and real level factors in the model. Using the same Treasury yield data, the stochastic volatility (SV) model exhibits similar in-sample fit and out-of-sample forecast performance relative to the constant volatility (CV) model. Specifically, the two models' transformations of their conditional mean specifications into such objects of interest as five-year inflation expectations and inflation risk premiums exhibit similar dynamics. In contrast, and more importantly for valuing the TIPS deflation protection option, the models exhibit important differences related to the transformations of their conditional volatility dynamics into conditional distributions of headline CPI changes.

In particular, the one-year deflation probability forecasts generated by the SV model are generally higher than those generated by the CV model. As might be expected, the differing deflation probabilities lead to important differences in the model-implied values of the TIPS deflation protection option. Figure 1 shows the yield spread between pairs of TIPS with

[2]Adrian and Wu (2010) also propose a model of nominal and real Treasury yields with spanned stochastic volatility. In related research, Haubrich et al. (2012) and Fleckenstein et al. (2013) build models of inflation swap rates with stochastic volatility.

similar maturities, but differing degrees of accumulated inflation protection. This spread is a proxy for the value of the embedded deflation protection option, as per Wright (2009). As shown in the figure, the SV model generates a yield spread that more directly captures the observed spread in the last few months of 2008 and into 2009. In fact, while both sets of model-implied spreads have correlations of nearly 0.9 with the observed spread, the SV model has a root mean squared error over 2009 of 9.5 basis points as compared to 28.7 basis points for the CV model. In 2008 before the Lehman bankruptcy, the SV model-implied value of the TIPS deflation protection option at the five-year maturity was 6.8 basis points. During the height of the crisis period in late 2008, that value jumped to 89.1 basis points as deflationary concerns rose markedly during the sharp economic contraction. For 2009 as a whole, the average value of this option was 41 basis points on a par-yield basis, and that average value declined to 19.5 for 2010. These results suggest that the SV model is well equipped to measure and price deflation risk within the Treasury market, and thus it should be well placed to price the inflation derivatives increasingly being traded in the United States.[3]

Finally, equipped with accurate estimates of the price of the embedded deflation protection option, we study the market factors that influence its value. Specifically, we use regressions to analyze the par-bond yield spread between a comparable seasoned and newly issued TIPS discussed above, which we refer to as the deflation risk premium. The empirical challenge is to assess what part of this deflation risk premium reflects outright deflation fears associated with general economic uncertainty and what part is a reflection of market illiquidity and limits to arbitrage.[4] Our primary explanatory factor to account for the former is the VIX options-implied volatility index, which represents near-term uncertainty about the general stock market and is widely used as a gauge of investor risk aversion. We also include variables that gauge market illiquidity, such as the economy-wide market illiquidity measure introduced by Hu et al. (2013, henceforth HPW). Our empirical results suggest that general economic uncertainty as reflected in the VIX is the main factor determining the deflation risk premium, accounting for about 65% of its observed variation. However, liquidity effects also play a role, particularly before and during the 2008-2009 financial crisis. Further research into this important aspect of TIPS pricing and liquidity premia is needed.

The paper is structured as follows. Section 2 introduces the general theoretical framework for inferring deflation dynamics from nominal and real Treasury yield curves and details our proposed methodology for deriving the model-implied value of the deflation protection option. Section 3 describes the term structure model with constant volatility as developed by CLR as well as the specification of the SV model used for this study. Section 4 contains the data description and the empirical results for the two models, while Section 5 analyzes the drivers

[3] See Christensen and Gillan (2012) for further discussion of U.S. inflation swaps and related liquidity issues. Kitsul and Wright (2013) examine inflation caps and floors to derive option-implied inflation probability density functions.

[4] TIPS liquidity has been a concern historically, and not least at the peak of the financial crisis, see CLR and Fleckenstein et al. (2012) for detailed discussions.

of the deflation risk premium. Section 6 concludes and provides directions for future research. The appendices contain additional technical details.

2 Pricing Deflation Risk with Treasuries and TIPS

In this section, we provide the theoretical foundation for the framework we use to price deflation protection options.

2.1 Deriving Market-Implied Inflation Expectations and Risk Premiums

An arbitrage-free term structure model can be used to decompose the difference between nominal and real Treasury yields, also known as the breakeven inflation (BEI) rate, into the sum of inflation expectations and an inflation risk premium. We follow Merton (1974) and assume a continuum of nominal and real zero-coupon Treasury bonds exist with no frictions to their continuous trading. The economic implication of this assumption is that the markets for inflation risk are complete in the limit. Define the nominal and real stochastic discount factors, denoted M_t^N and M_t^R, respectively. The no-arbitrage condition enforces a consistency of pricing for any security over time. Specifically, the price of a nominal bond that pays one dollar in τ years and the price of a real bond that pays one unit of the defined consumption basket in τ years must satisfy the conditions that

$$P_t^N(\tau) = E_t^P\left[\frac{M_{t+\tau}^N}{M_t^N}\right] \quad \text{and} \quad P_t^R(\tau) = E_t^P\left[\frac{M_{t+\tau}^R}{M_t^R}\right],$$

where $P_t^N(\tau)$ and $P_t^R(\tau)$ are the observed prices of the zero-coupon, nominal and real bonds for maturity τ on day t and $E_t^P[.]$ is the conditional expectations operator under the real-world (or P-) probability measure. The no-arbitrage condition also requires a consistency between the prices of real and nominal bonds such that the price of the consumption basket, denoted as the overall price level Π_t, is the ratio of the nominal and real stochastic discount factors:

$$\Pi_t = \frac{M_t^R}{M_t^N}.$$

We assume that the nominal and real stochastic discount factors have the standard dynamics given by

$$\begin{aligned} dM_t^N/M_t^N &= -r_t^N dt - \Gamma_t' dW_t^P, \\ dM_t^R/M_t^R &= -r_t^R dt - \Gamma_t' dW_t^P, \end{aligned}$$

where r_t^N and r_t^R are the instantaneous, risk-free nominal and real rates of return, respectively, and Γ_t is a vector of premiums on the risks represented by W_t^P. By Ito's lemma, the dynamic evolution of Π_t is given by

$$d\Pi_t = (r_t^N - r_t^R)\Pi_t dt.$$

Thus, with the absence of arbitrage, the instantaneous growth rate of the price level is equal to the difference between the instantaneous nominal and real risk-free rates.[5] Correspondingly, we can express the stochastic price level at time t+τ as

$$\Pi_{t+\tau} = \Pi_t e^{\int_t^{t+\tau}(r_s^N - r_s^R)ds}.$$

The relationship between the yields and inflation expectations can be obtained by decomposing the price of the nominal bond as follows:

$$\begin{aligned} P_t^N(\tau) &= E_t^P\left[\frac{M_{t+\tau}^N}{M_t^N}\right] = E_t^P\left[\frac{M_{t+\tau}^R/\Pi_{t+\tau}}{M_t^R/\Pi_t}\right] = E_t^P\left[\frac{M_{t+\tau}^R}{M_t^R}\frac{\Pi_t}{\Pi_{t+\tau}}\right] \\ &= E_t^P\left[\frac{M_{t+\tau}^R}{M_t^R}\right] \times E_t^P\left[\frac{\Pi_t}{\Pi_{t+\tau}}\right] + cov_t^P\left[\frac{M_{t+\tau}^R}{M_t^R}, \frac{\Pi_t}{\Pi_{t+\tau}}\right] \\ &= P_t^R(\tau) \times E_t^P\left[\frac{\Pi_t}{\Pi_{t+\tau}}\right] \times \left(1 + \frac{cov_t^P\left[\frac{M_{t+\tau}^R}{M_t^R}, \frac{\Pi_t}{\Pi_{t+\tau}}\right]}{E_t^P\left[\frac{M_{t+\tau}^R}{M_t^R}\right] \times E_t^P\left[\frac{\Pi_t}{\Pi_{t+\tau}}\right]}\right). \end{aligned}$$

Converting this price into a yield-to-maturity using

$$y_t^N(\tau) = -\frac{1}{\tau}\ln P_t^N(\tau) \quad \text{and} \quad y_t^R(\tau) = -\frac{1}{\tau}\ln P_t^R(\tau), \tag{1}$$

we obtain

$$y_t^N(\tau) = y_t^R(\tau) + \pi_t^e(\tau) + \phi_t(\tau), \tag{2}$$

where the market-implied rate of inflation expected at time t for the period from t to $t+\tau$ is

$$\pi_t^e(\tau) = -\frac{1}{\tau}\ln E_t^P\left[\frac{\Pi_t}{\Pi_{t+\tau}}\right] = -\frac{1}{\tau}\ln E_t^P\left[e^{-\int_t^{t+\tau}(r_s^N - r_s^R)ds}\right] \tag{3}$$

and the associated inflation risk premium for the same time period is

$$\phi_t(\tau) = -\frac{1}{\tau}\ln\left(1 + \frac{cov_t^P\left[\frac{M_{t+\tau}^R}{M_t^R}, \frac{\Pi_t}{\Pi_{t+\tau}}\right]}{E_t^P\left[\frac{M_{t+\tau}^R}{M_t^R}\right] \times E_t^P\left[\frac{\Pi_t}{\Pi_{t+\tau}}\right]}\right). \tag{4}$$

Note that this inflation risk premium can be positive or negative, while the deflation risk premium examined empirically in Section 5 is one-sided.

[5] We emphasize that the price level is a stochastic process as long as r_t^N and r_t^R are stochastic processes.

2.2 The Value of the Deflation Protection Embedded in TIPS

The primary focus of this paper is the value of the deflation protection embedded in TIPS and how, during the financial crisis of 2008 and 2009, it affected the relative prices of pairs of TIPS differentiated only by their accrued inflation compensation. Under standard inflationary conditions, the value of the deflation protection should not play an important role in TIPS pricing since the probability of having negative net accrued inflation compensation at maturity is negligible; that is, the option should be well out-of-the-money. However, at the peak of the financial crisis in the fall of 2008, neither the perceived nor the priced probability of deflation were negligible as we show in Section 4. Under these circumstances, a wedge can develop between the prices of seasoned TIPS with a significant amount of accrued inflation compensation and recently issued on-the-run TIPS, which have no cumulated inflation compensation. As suggested by Wright (2009), this wedge is a proxy for the value of the TIPS deflation protection option.

To examine the ability of the proposed models to price these deflation protection options, we use the models' implied yield curves and deflation probabilities. We calculate the deflation protection option values by comparing the prices of a newly issued TIPS without any accrued inflation compensation and a seasoned TIPS with sufficient accrued inflation compensation under the risk-neutral (or Q-) pricing measure. First, consider a hypothetical seasoned TIPS with T years remaining to maturity that pays an annual coupon C semi-annually. Assume this bond has accrued sufficient inflation compensation so it is nearly impossible to reach the deflation floor before maturity. Under the risk-neutral pricing measure, the par-coupon bond satisfying these criteria has a coupon rate determined by the equation

$$\sum_{i=1}^{2T} \frac{C}{2} E_t^Q \left[e^{-\int_t^{t_i} r_s^R ds} \right] + E_t^Q \left[e^{-\int_t^{T} r_s^R ds} \right] = 1. \tag{5}$$

The first term is the sum of the present value of the $2T$ coupon payments using the model's fitted real yield curve at day t. The second term is the discounted value of the principal payment. The coupon payment of the seasoned bond that solves this equation is denoted as C_S.

Next, consider a new TIPS with no accrued inflation compensation with T years to maturity. Since the coupon payments are not protected against deflation, the difference is in accounting for the deflation protection on the principal payment. For this bond, the pricing equation has an additional term; that is,

$$\sum_{i=1}^{2T} \frac{C}{2} E_t^Q \left[e^{-\int_t^{t_i} r_s^R ds} \right] + E_t^Q \left[\frac{\Pi_T}{\Pi_t} \cdot e^{-\int_t^{T} r_s^N ds} \mathbf{1}_{\{\frac{\Pi_T}{\Pi_t} > 1\}} \right] + E_t^Q \left[1 \cdot e^{-\int_t^{T} r_s^N ds} \mathbf{1}_{\{\frac{\Pi_T}{\Pi_t} \leq 1\}} \right] = 1.$$

The first term is the same as before. The second term represents the present value of the principal payment conditional on a positive net change in the price index over the bond's maturity; that is, $\frac{\Pi_T}{\Pi_t} > 1$. Under this condition, full inflation indexation applies, and the price change $\frac{\Pi_T}{\Pi_t}$ is placed within the expectations operator. The third term represents the present value of the *floored* TIPS principal conditional on accumulated net deflation; that is, when the price level change is below one, $\frac{\Pi_T}{\Pi_t}$ is replaced by a value of one to provide the promised deflation protection.

Since

$$\frac{\Pi_T}{\Pi_t} = e^{\int_t^T (r_s^N - r_s^R) ds},$$

the equation can be rewritten as

$$\sum_{i=1}^{2T} \frac{C}{2} E_t^Q [e^{-\int_t^{t_i} r_s^R ds}] + E_t^Q \Big[e^{-\int_t^T r_s^R ds} \Big] + \Bigg[E_t^Q \Big[e^{-\int_t^T r_s^N ds} \mathbf{1}_{\{\frac{\Pi_T}{\Pi_t} \leq 1\}} \Big] - E_t^Q \Big[e^{-\int_t^T r_s^R ds} \mathbf{1}_{\{\frac{\Pi_T}{\Pi_t} \leq 1\}} \Big] \Bigg] = 1,$$

where the last term on the left-hand side represents the net present value of the deflation protection of the principal in the TIPS contract. The par-coupon yield of a new hypothetical TIPS that solves this equation is denoted as C_0. The difference between C_S and C_0 is a measure of the advantage of being at the inflation adjustment floor for a newly issued TIPS and thus of the value of the embedded deflation protection option.

3 Models of Nominal and Real Treasury Yield Curves

Given the theoretical framework introduced in the previous section, we briefly summarize the affine term structure model of nominal and real Treasury yields with constant volatility developed by CLR and then introduce the modified version with stochastic yield volatility. Please note that even though the models are not formulated using the canonical form of affine term structure models introduced by Dai and Singleton (2000), both models can be viewed as restricted versions of their respective canonical model.[6] Furthermore, it can be noted that most of the restrictions imposed are motivated by a desire to generate a factor loading structure in the zero-coupon bond yield functions that closely matches the popular Nelson and Siegel (1987) model.

3.1 The Constant Volatility Model

The joint four-factor constant volatility (CV) model of nominal and real yields is a direct extension of the three-factor, arbitrage-free Nelson-Siegel (AFNS) model developed by Christensen, Diebold and Rudebusch (2011, henceforth CDR) for nominal yields. In the CV model, the state vector is denoted by $X_t = (L_t^N, S_t, C_t, L_t^R)$, where L_t^N is the level factor for nominal yields, S_t is the common slope factor, C_t is the common curvature factor, and L_t^R is the level

[6]These restrictions can be derived explicitly, and the calculations are available upon request.

factor for real yields.[7] The instantaneous nominal and real risk-free rates are defined as:

$$r_t^N = L_t^N + S_t, \tag{6}$$

$$r_t^R = L_t^R + \alpha^R S_t. \tag{7}$$

Note that the differential scaling of the real rates to the common slope factor is captured by the parameter α^R. To preserve the Nelson-Siegel factor loading structure in the yield functions, the risk-neutral (or Q-) dynamics of the state variables are given by the stochastic differential equations:[8]

$$\begin{pmatrix} dL_t^N \\ dS_t \\ dC_t \\ dL_t^R \end{pmatrix} = \begin{pmatrix} 0 & 0 & 0 & 0 \\ 0 & -\lambda & \lambda & 0 \\ 0 & 0 & -\lambda & 0 \\ 0 & 0 & 0 & 0 \end{pmatrix} \begin{pmatrix} L_t^N \\ S_t \\ C_t \\ L_t^R \end{pmatrix} dt + \Sigma \begin{pmatrix} dW_t^{L^N,Q} \\ dW_t^{S,Q} \\ dW_t^{C,Q} \\ dW_t^{L^R,Q} \end{pmatrix}, \tag{8}$$

where Σ is the constant covariance (or volatility) matrix.[9] Based on this specification of the Q-dynamics, nominal Treasury zero-coupon bond yields preserve the Nelson-Siegel factor loading structure as

$$y_t^N(\tau) = L_t^N + \left(\frac{1-e^{-\lambda\tau}}{\lambda\tau}\right) S_t + \left(\frac{1-e^{-\lambda\tau}}{\lambda\tau} - e^{-\lambda\tau}\right) C_t - \frac{A^N(\tau)}{\tau}, \tag{9}$$

where $A^N(\tau)/\tau$ is a maturity-dependent yield-adjustment term. Similarly, real TIPS zero-coupon bond yields have a Nelson-Siegel factor loading structure expressed as

$$y_t^R(\tau) = L_t^R + \alpha^R \left(\frac{1-e^{-\lambda\tau}}{\lambda\tau}\right) S_t + \alpha^R \left(\frac{1-e^{-\lambda\tau}}{\lambda\tau} - e^{-\lambda\tau}\right) C_t - \frac{A^R(\tau)}{\tau}. \tag{10}$$

Note that $A^R(\tau)/\tau$ is another maturity-dependent yield-adjustment term. These two equations, when combined in state-space form, constitute the measurement equation needed for Kalman filter estimation.

To complete the model, we define the price of risk, which links the risk-neutral and real-world yield dynamics, using the essentially affine risk premium specification introduced by Duffee (2002). The real-world dynamics of the state variables are then expressed as

$$dX_t = K^P(\theta^P - X_t)dt + \Sigma dW_t^P, \tag{11}$$

[7] Chernov and Mueller (2012) provide evidence of a hidden factor in the nominal yield curve that is observable from real yields and inflation expectations. Our models accommodate this stylized fact via the L_t^R factor.

[8] As discussed in CDR, with unit roots in the two level factors, the model is not arbitrage-free with an unbounded horizon; therefore, as is often done in theoretical discussions, we impose an arbitrary maximum horizon.

[9] As per CDR, Σ is a diagonal matrix, and θ^Q is set to zero without loss of generality.

which in its most general form can be written as[10]

$$\begin{pmatrix} dL_t^N \\ dS_t \\ dC_t \\ dL_t^R \end{pmatrix} = \begin{pmatrix} \kappa_{11}^P & \kappa_{12}^P & \kappa_{13}^P & \kappa_{14}^P \\ \kappa_{21}^P & \kappa_{22}^P & \kappa_{23}^P & \kappa_{24}^P \\ \kappa_{31}^P & \kappa_{32}^P & \kappa_{33}^P & \kappa_{34}^P \\ \kappa_{41}^P & \kappa_{42}^P & \kappa_{43}^P & \kappa_{44}^P \end{pmatrix} \left(\begin{pmatrix} \theta_1^P \\ \theta_2^P \\ \theta_3^P \\ \theta_4^P \end{pmatrix} - \begin{pmatrix} L_t^N \\ S_t \\ C_t \\ L_t^R \end{pmatrix} \right) dt + \Sigma \begin{pmatrix} dW_t^{L^N,P} \\ dW_t^{S,P} \\ dW_t^{C,P} \\ dW_t^{L^R,P} \end{pmatrix}. \quad (12)$$

This equation is the transition equation used in the Kalman filter estimation.

3.2 The Stochastic Volatility Model

Financial time series, such as interest rates and bond yields, have been shown to have time-varying volatility, which is a feature not often incorporated into arbitrage-free term structure models; see Andersen and Benzoni (2010) for further discussion. To address this concern, Christensen et al. (2014a) develop a general class of AFNS models that incorporate spanned stochastic volatility. To distinguish between the various types of models, we use the notation outlined in Dai and Singleton (2000) for classifying affine term structure models, such that the CV model is within the $A_0(4)$ class of models that do not have volatility dynamics. As detailed in Christensen et al. (2014a), there are several possible volatility specifications within their three-factor framework, and clearly, the introduction of the fourth factor within the CLR model generates an even larger set of possible specifications.

For this paper, we chose an $A_2(4)$ volatility specification that incorporates stochastic volatility based on the nominal and real level factors. This choice was motivated by a desire to focus on the longer maturity TIPS yields, since observable proxies for the value of the TIPS deflation protection option are most available near the five-year maturity point.[11] For this stochastic volatility (SV) model, the state vector and instantaneous risk-free rates are the same as before. To preserve the Nelson-Siegel factor loading structure and impose our volatility specification, the Q-dynamics of the state variables are given by[12]

$$\begin{pmatrix} dL_t^N \\ dS_t \\ dC_t \\ dL_t^R \end{pmatrix} = \begin{pmatrix} \kappa_{L^N}^Q & 0 & 0 & 0 \\ 0 & \lambda & -\lambda & 0 \\ 0 & 0 & \lambda & 0 \\ 0 & 0 & 0 & \kappa_{L^R}^Q \end{pmatrix} \left[\begin{pmatrix} \theta_{L^N}^Q \\ 0 \\ 0 \\ \theta_{L^R}^Q \end{pmatrix} - \begin{pmatrix} L_t^N \\ S_t \\ C_t \\ L_t^R \end{pmatrix} \right] dt \quad (13)$$

[10] The model specification given by Equations (6), (7), (8), and (12) has 14 restrictions relative to its canonical $A_0(4)$ model.

[11] Please note that the empirical results for the $A_1(4)$ specifications using just the nominal or real level factors are qualitatively similar, although quantitatively worse than the $A_2(4)$ specification. These results are available upon request.

[12] While the modeling framework allows for the two level factors to directly affect the volatility of the common slope and curvature factors, we fix the associated volatility sensitivity parameters to zero as per Christensen et al. (2014a), who report that these volatility sensitivity parameters are typically insignificant for U.S. Treasury data. This choice leads to analytical bond pricing formulas that greatly facilitate model estimation and analysis.

$$
+\begin{pmatrix} \sigma_{11} & 0 & 0 & 0 \\ 0 & \sigma_{22} & 0 & 0 \\ 0 & 0 & \sigma_{33} & 0 \\ 0 & 0 & 0 & \sigma_{44} \end{pmatrix} \begin{pmatrix} \sqrt{L_t^N} & 0 & 0 & 0 \\ 0 & \sqrt{1} & 0 & 0 \\ 0 & 0 & \sqrt{1} & 0 \\ 0 & 0 & 0 & \sqrt{L_t^R} \end{pmatrix} \begin{pmatrix} dW_t^{L^N,Q} \\ dW_t^{S,Q} \\ dW_t^{C,Q} \\ dW_t^{L^R,Q} \end{pmatrix}.
$$

The representation of the nominal zero-coupon bond yield function becomes

$$
y_t^N(\tau) = g^N\left(\kappa_{L^N}^Q\right)L_t^N + \left(\frac{1-e^{-\lambda\tau}}{\lambda\tau}\right)S_t + \left(\frac{1-e^{-\lambda\tau}}{\lambda\tau} - e^{-\lambda\tau}\right)C_t - \frac{A^N\left(\tau;\kappa_{L^N}^Q\right)}{\tau}, \tag{14}
$$

where $g^N\left(\kappa_{L^N}^Q\right)$ is a modified loading on the nominal level factor.[13] Note that the slope and the curvature factor preserve their Nelson-Siegel factor loadings exactly, although the structure of the yield-adjustment term $A^N\left(\tau;\kappa_{L^N}^Q\right)/\tau$ is different than before. Correspondingly, the real zero-coupon bond yield function is now

$$
y_t^R(\tau) = g^R\left(\kappa_{L^R}^Q\right)L_t^R + \alpha^R\left(\frac{1-e^{-\lambda\tau}}{\lambda\tau}\right)S_t + \alpha^R\left(\frac{1-e^{-\lambda\tau}}{\lambda\tau} - e^{-\lambda\tau}\right)C_t - \frac{A^R\left(\tau;\kappa_{L^R}^Q\right)}{\tau}, \tag{15}
$$

where $g^R\left(\kappa_{L^R}^Q\right)$ is a modified loading on the real level factor and $A^R\left(\tau;\kappa_{L^R}^Q\right)/\tau$ is a modified yield-adjustment term.[14]

To link the risk-neutral and real-world dynamics of the state variables, we here use the extended affine risk premium specification introduced by Cheridito et al. (2007), as per Christensen et al. (2014a). The maximally flexible affine specification of the P-dynamics is thus[15]

$$
\begin{pmatrix} dL_t^N \\ dS_t \\ dC_t \\ dL_t^R \end{pmatrix} = \begin{pmatrix} \kappa_{11}^P & 0 & 0 & \kappa_{14}^P \\ \kappa_{21}^P & \kappa_{22}^P & \kappa_{23}^P & \kappa_{24}^P \\ \kappa_{31}^P & \kappa_{32}^P & \kappa_{33}^P & \kappa_{34}^P \\ \kappa_{41}^P & 0 & 0 & \kappa_{44}^P \end{pmatrix} \left[\begin{pmatrix} \theta_1^P \\ \theta_2^P \\ \theta_3^P \\ \theta_4^P \end{pmatrix} - \begin{pmatrix} L_t^N \\ S_t \\ C_t \\ L_t^R \end{pmatrix}\right] dt \tag{16}
$$

$$
+\begin{pmatrix} \sigma_{11} & 0 & 0 & 0 \\ 0 & \sigma_{22} & 0 & 0 \\ 0 & 0 & \sigma_{33} & 0 \\ 0 & 0 & 0 & \sigma_{44} \end{pmatrix} \begin{pmatrix} \sqrt{L_t^N} & 0 & 0 & 0 \\ 0 & \sqrt{1} & 0 & 0 \\ 0 & 0 & \sqrt{1} & 0 \\ 0 & 0 & 0 & \sqrt{L_t^R} \end{pmatrix} \begin{pmatrix} dW_t^{L^N,P} \\ dW_t^{S,P} \\ dW_t^{C,P} \\ dW_t^{L^R,P} \end{pmatrix}.
$$

To keep the model arbitrage-free, the two level factors must be prevented from hitting the lower zero-boundary. This positivity requirement is ensured by imposing the Feller conditions

[13] Analytical formulas for $g^N\left(\kappa_{L^N}^Q\right)$, $g^R\left(\kappa_{L^R}^Q\right)$, $A^N\left(\tau;\kappa_{L^N}^Q\right)$, and $A^R\left(\tau;\kappa_{L^R}^Q\right)$ are provided in Appendix A.

[14] In our implementation, we fix $\kappa_{L^N}^Q = \kappa_{L^R}^Q = 10^{-7}$ to get a close approximation to the uniform level factor loading in the CV model.

[15] The specification given by Equations (6), (7), (13), and (16) has 20 restrictions relative to its canonical $A_2(4)$ model.

under both probability measures, which in this case are four; that is,

$$\kappa_{11}^P \theta_1^P + \kappa_{14}^P \theta_4^P > \frac{1}{2}\sigma_{11}^2,$$

$$10^{-7} \cdot \theta_{L^N}^Q > \frac{1}{2}\sigma_{11}^2,$$

$$\kappa_{41}^P \theta_1^P + \kappa_{44}^P \theta_4^P > \frac{1}{2}\sigma_{44}^2,$$

and

$$10^{-7} \cdot \theta_{L^R}^Q > \frac{1}{2}\sigma_{44}^2.$$

Furthermore, to have well-defined processes for L_t^N and L_t^R, the sign of the effect that these two factors have on each other must be positive, which requires the restrictions that

$$\kappa_{14}^P \leq 0 \quad \text{and} \quad \kappa_{41}^P \leq 0.$$

These conditions ensure that the two square-root processes will be non-negatively correlated.[16]

3.2.1 Deflation Probabilities within the SV Model

Christensen et al. (2012) use the CV model to generate deflation probabilities at various horizons appropriate for macroeconomic and monetary policy purposes. Similarly, the SV model can be used to calculate deflation probabilities, although additional steps are necessary.

The change in the price index implied by the model's "yields-only" approach for the period from t to $t+\tau$ is given by

$$\frac{\Pi_{t+\tau}}{\Pi_t} = e^{\int_t^{t+\tau}(r_s^N - r_s^R)ds}.$$

To determine whether the change in the price index over a τ-period horizon may be below a critical level q, we are interested in the probability of the states where

$$\frac{\Pi_{t+\tau}}{\Pi_t} \leq 1+q,$$

or, equivalently,

$$Y_{t,\tau} = \int_t^{t+\tau}(r_s^N - r_s^R)ds \leq \ln(1+q).$$

Given that $r_t^N = L_t^N + S_t$ and $r_t^R = L_t^R + \alpha^R S_t$, we are interested in the distributional

[16] Our empirical results show that the Feller condition pertaining to the real yield level factor L_t^R under the Q-measure is systematically binding, while the other three Feller conditions are never binding. Thus, it is mainly the dynamics of L_t^R that are affected by the imposition of the Feller conditions, most notably σ_{44}. For robustness, we analyzed the specification of the SV model without Feller conditions imposed, but found it to underperform along multiple dimensions relative to the reported SV model with Feller conditions imposed. Results for this alternative specification and analysis are available upon request.

properties of the process

$$Y_{0,t} = \int_0^t (r_s^N - r_s^R)ds = \int_0^t (L_s^N + S_s - L_s^R - \alpha^R S_s)ds \quad \Rightarrow \quad dY_{0,t} = (L_t^N + (1-\alpha^R)S_t - L_t^R)dt.$$

This process is then introduced into the system of equations containing the P-dynamics of the state variables X_t.

Due to the introduction of stochastic volatility into the two level factors, this system of equations no longer has Gaussian state variables. As a consequence, we must use the Fourier transform analysis described in full generality for affine models in Duffie, Pan, and Singleton (2000), as opposed to the approach detailed in Christensen et al. (2012) for the CV model. The intuition of this approach is to express expectations of contingent payments in a tractable, mathematical form. By simplifying these expectations to indicator variables such as $\mathbf{1}_{(Y_{t,\tau} \leq \ln(1+q))}$, event probabilities are readily generated; see Appendix C for details.

3.3 Model Estimation

As noted above, the SV model is non-Gaussian, which prevents us from using some of the recently proposed estimation techniques, such as Joslin et al (2011). Instead, the estimation of both models relies on the Kalman filter as in CLR and Christensen et al. (2012); that is, nominal and real zero-coupon yields are affine functions of the state variables such that

$$y_t(\tau) = -\frac{1}{\tau}B(\tau)'X_t - \frac{1}{\tau}A(\tau) + \varepsilon_t(\tau),$$

where $\varepsilon_t(\tau)$ are assumed to be i.i.d. Gaussian errors. The conditional mean for multi-dimensional affine diffusion processes is given by

$$E^P[X_T|X_t] = (I - \exp(-K^P(T-t)))\theta^P + \exp(-K^P(T-t))X_t, \tag{17}$$

where $\exp(-K^P(T-t))$ is a matrix exponential. In general, the conditional covariance matrix for affine diffusion processes is given by

$$V^P[X_T|X_t] = \int_t^T \exp(-K^P(T-s))\Sigma D(E^P[X_s|X_t])D(E^P[X_s|X_t])'\Sigma' \exp(-(K^P)'(T-s))ds. \tag{18}$$

Stationarity of the system under the P-measure is ensured if the real components of all the eigenvalues of K^P are positive, and this condition is imposed in all estimations. For this reason, we can start the Kalman filter at the unconditional mean and covariance matrix.[17] However, the introduction of stochastic volatility in the SV model implies that the factors are no longer Gaussian since their variances are now dependent on the path of the state

[17] In the estimation, we calculate the conditional and unconditional covariance matrices using the analytical solutions provided in Fisher and Gilles (1996), which differs from the previous studies by CLR and Christensen et al. (2012) that relied upon numerical approximations.

variables. For tractability, we choose to approximate the true probability distribution of the state variables using the first and second moments described above and use the Kalman filter algorithm *as if* the state variables were Gaussian.[18] The state equation is given by

$$X_t = (I - \exp(-K^P \Delta t))\theta^P + \exp(-K^P \Delta t) X_{t-1} + \eta_t, \quad \eta_t \sim N(0, V_{t-1}),$$

where Δt is the time between observations and V_{t-1} is the conditional covariance matrix given in Equation (18).[19] In the Kalman filter estimations, the error structure is given by

$$\begin{pmatrix} \eta_t \\ \varepsilon_t \end{pmatrix} \sim N\left[\begin{pmatrix} 0 \\ 0 \end{pmatrix}, \begin{pmatrix} V_{t-1} & 0 \\ 0 & H \end{pmatrix}\right],$$

where H is assumed to be a diagonal matrix of the measurement error standard deviations, $\sigma_\varepsilon(\tau_i)$, that are specific to each yield maturity in the data set. Furthermore, the discrete nature of the transition equation can cause the square-root processes to become negative despite the fact that the parameter sets are forced to satisfy Feller conditions and other non-negativity restrictions. Whenever this happens, we follow the literature and simply truncate those processes at zero; see Duffee (1999) for an example.

4 Empirical Analysis

In this section, we first detail the data used for model estimation before describing the estimation results with particular emphasis on the risk of deflation and its implications for the value of the deflation protection options embedded in TIPS.

4.1 Data

In this paper, the nominal Treasury bond yields used are zero-coupon yields constructed as in Gürkaynak et al. (2007).[20] These yields are constructed using a discount function of the Svensson (1995)-type to minimize the pricing error of a large pool of underlying off-the-run Treasury bonds. As demonstrated by Gürkaynak et al. (2007), the model fits the underlying pool of bond prices extremely well. By implication, the zero-coupon yields derived from this approach constitute a very good approximation of the underlying Treasury zero-coupon yield

[18] A few notable examples of papers that follow this approach include Duffee (1999), Driessen (2005), and Feldhütter and Lando (2008). An unreported simulation analysis suggests that the added bias from using the Kalman filter in estimating the SV model is modest relative to the finite-sample bias that even the CV model is subject to.

[19] For estimation purposed over the first eight years of the sample without TIPS yields, $e^{-K^P \Delta t}$, $(1 - e^{-K^P \Delta t})\theta^P$, and the conditional covariance matrix $\int_t^{t+\tau} e^{-K^P(t+\tau-s)} \Sigma D(E^P[X_s|X_t]) D(E^P[X_s|X_t])' \Sigma' e^{-(K^P)'(t+\tau-s)} ds$ are calculated using the upper (3×3) part of K^P and the upper (3×1) part of θ^P.

[20] The Board of Governors of the Federal Reserve updates the data on its website at http://www.federalreserve.gov/pubs/feds/2006/index.html.

curve. From this dataset, we use eight Treasury zero-coupon bond yields with maturities of 3-months, 6-months, 1-year, 2-years, 3-years, 5-years, 7-years, and 10-years. We use weekly Friday data and limit our sample to the period from January 6, 1995, to December 31, 2010, which provides us with 835 weekly observations.[21] Similarly, for the real Treasury yields, we use the zero-coupon bond yields constructed with the same method used by Gürkaynak et al. (2010).[22] The data is available from January 1999, but due to weak liquidity in the first years of TIPS trading, we follow CLR and limit our sample to the period after 2002. We have weekly real Treasury yields from January 2, 2003, to December 31, 2010, a total of 418 observations. Since our focus is on the long-term real yields, we use the six yearly maturities from five to ten years.

4.2 Estimation Results

To select the best fitting specifications of each model's real-world dynamics, we use a general-to-specific modeling strategy that restricts the least significant parameter in the estimation to zero and then re-estimates the model. This strategy of eliminating the least significant coefficients is carried out down to the most parsimonious specification, which has a diagonal K^P matrix. The final specification choice is based on the values of the Akaike and Bayes information criteria as per CLR.[23]

For the CV model, the summary statistics of the model selection process are reported in Table 1. Both information criteria are minimized by specification (9), which has a K^P matrix specified as

$$K^P_{CV} = \begin{pmatrix} \kappa^P_{11} & 0 & 0 & 0 \\ \kappa^P_{21} & \kappa^P_{22} & \kappa^P_{23} & 0 \\ 0 & 0 & \kappa^P_{33} & 0 \\ \kappa^P_{41} & \kappa^P_{42} & 0 & \kappa^P_{44} \end{pmatrix}.$$

Table 2 contains the estimated parameters for this specification. All the off-diagonal elements are highly significant and consistent with the empirical results reported in CLR.[24] In terms of dynamic properties, the nominal level factor is a persistent, slowly varying process not affected by any of the other factors. The common curvature factor is also unaffected by the other factors, but is less persistent and more volatile. The common slope factor is in between these two extremes as it is less persistent than the nominal level factor and less volatile than

[21] We end the sample in 2010 to avoid having to address the complex problem of respecting the zero lower bound for nominal yields, which appears to have been severe since August 2011 when the FOMC first provided explicit forward guidance for future monetary policy. To support the view that this was less critical in 2009 and 2010, we point to Swanson and Williams (2014), who provide evidence that medium- and long-term Treasury yields responded to economic news during those two years in much the same way as in the prior decades.

[22] This dataset is also maintained by the Board of Governors of the Federal Reserve System at http://www.federalreserve.gov/pubs/feds/2008/index.html.

[23] See Harvey (1989) for further details.

[24] The primary difference with the specification favored by CLR is that the κ^P_{14} parameter is set to zero in this case.

Alternative specifications	Goodness-of-fit statistics				
	Max log L	k	p-value	AIC	BIC
(1) Unrestricted K^P	52,561.05	40	n.a.	-105,042.1	-104,853.0
(2) $\kappa_{24}^P = 0$	52,560.99	39	0.7290	-105,044.0	-104,859.6
(3) $\kappa_{24}^P = \kappa_{32}^P = 0$	52,560.89	38	0.6547	-105,045.8	-104,866.1
(4) $\kappa_{24}^P = \kappa_{32}^P = \kappa_{43}^P = 0$	52,560.76	37	0.6101	-105,047.5	-104,872.6
(5) $\kappa_{24}^P = \ldots = \kappa_{12}^P = 0$	52,560.58	36	0.5485	-105,049.2	-104,879.0
(6) $\kappa_{24}^P = \ldots = \kappa_{13}^P = 0$	52,560.52	35	0.7290	-105,051.0	-104,885.6
(7) $\kappa_{24}^P = \ldots = \kappa_{14}^P = 0$	52,559.97	34	0.2943	-105,051.9	-104,891.2
(8) $\kappa_{24}^P = \ldots = \kappa_{31}^P = 0$	52,559.40	33	0.2857	-105,052.8	-104,896.8
(9) $\kappa_{24}^P = \ldots = \kappa_{34}^P = 0$	52,558.84	32	0.2899	**-105,053.7**	**-104,902.4**
(10) $\kappa_{24}^P = \ldots = \kappa_{21}^P = 0$	52,549.96	31	< 0.0001	-105,037.9	-104,891.4
(11) $\kappa_{24}^P = \ldots = \kappa_{42}^P = 0$	52,542.19	30	0.0001	-105,024.4	-104,882.6
(12) $\kappa_{24}^P = \ldots = \kappa_{41}^P = 0$	52,533.33	29	< 0.0001	-105,008.7	-104,871.6
(13) $\kappa_{24}^P = \ldots = \kappa_{23}^P = 0$	52,516.58	28	< 0.0001	-104,977.2	-104,844.8

Table 1: **Evaluation of Alternative Specifications of the CV Model.**
Thirteen alternative estimated specifications of the CV model of nominal and real Treasury bond yields are evaluated. Each specification is listed with its maximum log likelihood (Max $\log L$), number of parameters (k), the p-value from a likelihood ratio test of the hypothesis that the specification differs from the one directly above that has one more free parameter. The information criteria (AIC and BIC) are also reported, and their minimum values are given in boldface.

K^P	$K_{\cdot,1}^P$	$K_{\cdot,2}^P$	$K_{\cdot,3}^P$	$K_{\cdot,4}^P$	θ^P		Σ
$K_{1,\cdot}^P$	0.3483	0	0	0	0.0637	σ_{11}	0.0059
	(0.2528)				(0.0045)		(0.0002)
$K_{2,\cdot}^P$	1.4559	0.8185	-0.8148	0	-0.0289	σ_{22}	0.0087
	(0.4738)	(0.1678)	(0.1152)		(0.0174)		(0.0002)
$K_{3,\cdot}^P$	0	0	0.5416	0	-0.0175	σ_{33}	0.0297
			(0.2897)		(0.0135)		(0.0006)
$K_{4,\cdot}^P$	-4.1070	-0.6406	0	3.1116	0.0372	σ_{44}	0.0068
	(0.5491)	(0.1874)		(0.3428)	(0.0047)		(0.0001)

Table 2: **Parameter Estimates for the Preferred CV Model.**
The estimated parameters of the K^P matrix, θ^P vector, and diagonal Σ matrix are shown for the specification of the CV model preferred according to both AIC and BIC information criteria. The estimated value of λ is 0.5016 (0.0034), while α^R is estimated to be 0.5600 (0.0056). The numbers in parentheses are the estimated parameter standard deviations. The maximum log likelihood value is 52,558.84.

the curvature factor. Finally, the real level factor is the least persistent factor likely due to the shorter sample of real yields.

Turning to the chosen specification of the SV model, Table 3 contains the summary statistics of the model selection. For reasons of parsimony, we choose to focus on the specification

Alternative specifications	Goodness-of-fit statistics				
	Max log L	k	p-value	AIC	BIC
(1) Unrestricted K^P	54,479.99	38	n.a.	-108,884.0	-108,704.3
(2) $\kappa_{34}^P = 0$	54,479.99	37	1.0000	-108,886.0	-108,711.1
(3) $\kappa_{34}^P = \kappa_{24}^P = 0$	54,479.85	36	0.5967	-108,887.7	-108,717.5
(4) $\kappa_{34}^P = \kappa_{24}^P = \kappa_{31}^P = 0$	54,479.26	35	0.2774	-108,888.5	-108,723.1
(5) $\kappa_{34}^P = \ldots = \kappa_{32}^P = 0$	54,479.12	34	0.5967	**-108,890.2**	-108,729.5
(6) $\kappa_{34}^P = \ldots = \kappa_{21}^P = 0$	54,477.19	33	0.0495	-108,888.4	-108,732.4
(7) $\kappa_{34}^P = \ldots = \kappa_{41}^P = 0$	54,473.33	32	0.0055	-108,882.7	-108,731.4
(8) $\kappa_{34}^P = \ldots = \kappa_{14}^P = 0$	54,470.80	31	0.0245	-108,879.6	**-108,733.0**
(9) $\kappa_{31}^P = \ldots = \kappa_{23}^P = 0$	54,437.41	30	< 0.0001	-108,814.8	-108,673.0

Table 3: **Evaluation of Alternative Specifications of the SV Model**
Nine alternative estimated specifications of the SV model of nominal and real Treasury bond yields are evaluated. Each specification is listed with its log likelihood (Max log L), number of parameters (k), the p-value from a likelihood ratio test of the hypothesis that the specification differs from the one directly above that has one more free parameter. The information criteria (AIC and BIC) are also reported, and their minimum values are given in boldface.

preferred according to BIC with a mean-reversion matrix given by

$$K_{SV}^P = \begin{pmatrix} \kappa_{11}^P & 0 & 0 & 0 \\ 0 & \kappa_{22}^P & \kappa_{23}^P & 0 \\ 0 & 0 & \kappa_{33}^P & 0 \\ 0 & 0 & 0 & \kappa_{44}^P \end{pmatrix}.$$

Compared to the preferred specification of the CV model, κ_{21}^P and κ_{41}^P are jointly only borderline significant, while κ_{42}^P is not admissible.

The estimated parameters for this preferred specification are reported in Table 4. The most notable difference relative to the results for the CV model is that the nominal level factor is less persistent, while the real level factor is more persistent. Furthermore, for obvious reasons, σ_{11} and σ_{44} operate at different levels now due to the introduction of stochastic volatility through the first and fourth factor. However, as we show below, these differences do not lead to major differences in the models' first moment dynamics.

Table 5 contains summary statistics for the fitted errors from both models. For the nominal yields, the CV model fits the very short end of the nominal yield curve relatively better than the longer maturities in the one- to ten-year maturity range. In contrast, the SV model provides a better in-sample fit in the one- to ten-year maturity range, but less accurate fit for short-maturity yields. For the real yields, though, the SV model provides a significant overall improvement in model fit relative to the CV model, which is the main cause for the large difference in likelihood values.

In the following, we analyze the performance of the two models in greater detail using real-time analysis that adds one week of additional data to the estimation sample for each model

K^P	$K^P_{\cdot,1}$	$K^P_{\cdot,2}$	$K^P_{\cdot,3}$	$K^P_{\cdot,4}$	θ^P		Σ
$K^P_{1,\cdot}$	1.0431	0	0	0	0.0425	σ_{11}	0.0633
	(0.4193)				(0.0045)		(0.0006)
$K^P_{2,\cdot}$	0	0.6711	-0.6248	0	-0.0118	σ_{22}	0.0130
		(0.1867)	(0.1549)		(0.0143)		(0.0003)
$K^P_{3,\cdot}$	0	0	0.6915	0	-0.0076	σ_{33}	0.0303
			(0.1966)		(0.0119)		(0.0007)
$K^P_{4,\cdot}$	0	0	0	1.4203	0.0168	σ_{44}	0.0597
				(0.1914)	(0.0017)		(0.0007)

Table 4: **Parameter Estimates for the Preferred SV Model.**
The estimated parameters of the K^P matrix, the θ^P vector, and the Σ matrix for the preferred specification of the SV model according to BIC. The Q-related parameters are estimated at: $\lambda = 0.6067$ (0.0025), $\alpha^R = 0.4397$ (0.0068), $\theta^Q_{L^N} =$ 32,419 (31.67), and $\theta^Q_{L^R} =$ 17,846 (47.15). The numbers in parentheses are the estimated standard deviations of the parameter estimates. The maximum log likelihood value is 54,470.80.

Maturity in months	CV model			SV model		
Nom. yields	Mean	RMSE	$\widehat{\sigma}_\varepsilon(\tau_i)$	Mean	RMSE	$\widehat{\sigma}_\varepsilon(\tau_i)$
3	-0.54	9.53	9.51	0.75	19.23	19.22
6	0.00	0.00	0.00	-0.17	8.23	8.24
12	1.79	5.80	5.79	0.00	0.00	0.00
24	2.22	3.98	4.00	0.46	1.56	1.56
36	0.00	0.13	0.55	0.00	0.00	0.00
60	-2.67	3.73	3.83	-0.28	1.27	1.38
84	0.08	3.37	3.66	0.24	0.59	1.14
120	9.53	12.03	12.15	-1.15	4.41	4.59
TIPS yields	Mean	RMSE	$\widehat{\sigma}_\varepsilon(\tau_i)$	Mean	RMSE	$\widehat{\sigma}_\varepsilon(\tau_i)$
60	-3.98	20.27	20.20	-2.04	13.59	13.59
72	-2.60	12.23	12.18	-0.51	5.87	5.86
84	-1.31	5.64	5.61	0.00	0.00	0.00
96	0.00	0.00	0.00	-0.38	4.72	4.72
108	1.35	4.94	4.90	-1.52	8.74	8.74
120	2.74	9.32	9.25	-3.32	12.35	12.35
Max log L	52,558.84			54,470.80		

Table 5: **Summary Statistics of the Fitted Errors.**
The mean and root mean squared fitted errors (RMSE) for the preferred specification of the CV and SV models are shown. All numbers are measured in basis points. The nominal yields cover the period from January 6, 1995, to December 31, 2010, while the real TIPS yields cover the period from January 3, 2003, to December 31, 2010.

estimation; that is, each model is estimated using the sample covering the twelve-year period from January 6, 1995, to January 5, 2007, and relevant model output is calculated; then, one week of data is added to the sample and the models are re-estimated, and another set of model output is constructed. This process is continued until the sample ends on December

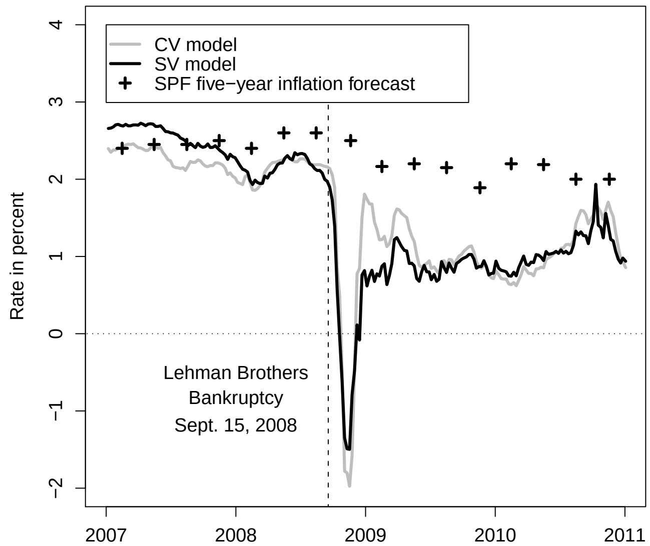

Figure 2: **Estimated Five-Year Inflation Expectations.**
Illustration of the estimated inflation expectations at the five-year horizon according to the CV and SV models. Included is the median five-year forecast of CPI inflation from the Survey of Professional Forecasters.

31, 2010.

4.3 Inflation Expectations

A key purpose of our joint models of nominal and real yields is to decompose BEI rates into inflation expectations and inflation risk premiums for further analysis. To conduct this analysis, we generate real-time, out-of-sample forecasts based on the rolling model estimation procedure described previously.

Figure 2 illustrates the models' market-implied expected inflation at the five-year horizon as well as the median of the five-year CPI inflation forecast from the Survey of Professional Forecasters (SPF). The preferred CV and SV models produce sharp declines in expected inflation shortly after the Lehman bankruptcy in September 2008, which is consistent with realized inflation; that is, headline CPI did register negative year-over-year changes during 2009 for the first time since 1955. Since the beginning of 2009, the two models suggest that medium-term inflation expectations have stabilized, but at a lower level than what prevailed prior to the financial crisis. This downward shift is consistent with the downward trend in the SPF survey measure, but notably larger. Furthermore, it appears consistent with the trend in CPI realizations, which has shifted down.[25]

[25]From the beginning of 2006 until the end of June 2008, the average annual rate of headline CPI inflation

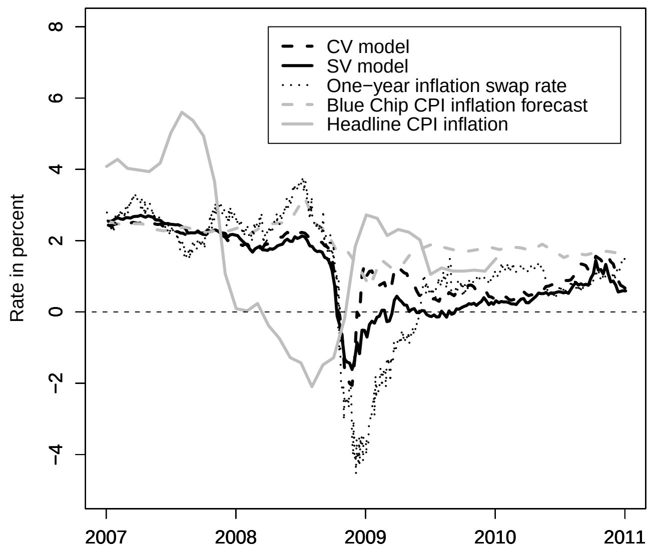

Figure 3: **One-Year CPI Inflation Forecasts.**
Illustration of year-over-year headline CPI inflation realizations are shown with a solid grey line. The one-year inflation forecasts from the CV and SV models are shown with a dashed and solid black line, respectively. Included are also the monthly Blue Chip one-year headline CPI inflation forecast (dashed grey line) and the one-year zero-coupon inflation swap rate downloaded from Bloomberg (dotted black line).

In Figure 3, the one-year inflation forecasts from the two models are compared to the subsequent headline CPI realizations as well as the corresponding survey forecasts provided by Blue Chip and the one-year inflation swap rate. Please note that both models and surveys are unable to capture the large variation in headline CPI inflation. To compare the various forecasts, Table 6 reports the results of aligning the model-generated inflation forecasts with the release dates of the Blue Chip survey and calculating the forecast errors for the 36 months from January 2007 through December 2009. In terms of matching headline CPI inflation, the two models are at least on par with, if not ahead of, the Blue Chip survey forecasts and the one-year inflation swap rate as measured by RMSEs.

In addition to the conditional expectations for future inflation studied so far, we also analyze the models' ability to match the unconditional moments of the CPI inflation process. To do so, we calculate the unconditional mean and standard deviation of the one- and two-year expected inflation from the two models and compare them to the corresponding statistics for headline CPI inflation realizations since January 2000. The results are reported in Table 7. Interestingly, the unconditional mean from the CV and SV models are below the mean of

was $\log(218.815/195.3)/2.5 = 4.5$ percent, while the average annual rate from mid-2008 through 2010 was a modest $\log(219.179/218.815)/2.5 = 0.1$ percent.

Model	Mean	RMSE
Random Walk	-39.35	349.34
Inflation swap	-38.86	224.45
Blue Chip	42.12	300.47
CV model	23.77	215.78
SV model	46.29	225.06

Table 6: **Comparison of Real-Time CPI Inflation Forecasts.**
Summary statistics for one-year forecast errors of headline CPI inflation in real time. The Blue Chip forecasts are mapped to the tenth of each month January 2007 to December 2009, a total of 36 monthly forecasts. The comparable model forecast is generated on the nearest available business day prior to the Blue Chip release. A similar principle is used for the collection of the corresponding inflation swap rate forecast. The subsequent CPI realizations are year-over-year changes starting at the end of the survey month. As a consequence, the random walk forecasts equal the past year-over-year change in the CPI series as of the end of the survey month.

Model	Unconditional distribution of $\pi_t^e(\tau)$			
	$\tau = 1$ year		$\tau = 2$ years	
	Mean	Std. dev.	Mean	Std. dev.
Headline CPI inflation	2.45	1.38	2.47	0.86
CV model	1.35	0.71	1.35	0.64
SV model	1.91	1.30	1.90	1.00

Table 7: **Moments from the Unconditional Distribution of Expected Inflation.**
The mean and standard deviation of the unconditional distribution of the one- and two-year expected inflation from the CV and SV models are shown. The parameters in each case are those estimated as of December 31, 2010. The mean and standard deviation of the unconditional distribution of expected headline CPI inflation outcomes are approximated by the mean and standard deviation of the monthly one- and two-year headline CPI inflation realizations over the period from January 2000 until December 2010, a total of 132 observations, measured at a continuously compounded rate. All numbers are measured in percent.

observed CPI realizations. However, in terms of the volatility of the price inflation process, the SV model is able to match the observed values very closely, while the CV model generates a distribution for inflation outcomes that is too narrow. This result suggests that the SV model captures price inflation dynamics reasonably well, in particular inflation uncertainty, even though no price indexes are used in the model estimation.

4.4 Deflation Probability Forecasts

Another relevant comparison measure for these models is their implied probability forecasts of net deflation one year ahead, as presented in Christensen et al. (2012) and in Figure 4. The risk of deflation in 2007 and leading up to the failure of Lehman Brothers in September 2008 was basically zero under both models. In late 2008, the models assigned a high probability to net deflation over the following twelve-month period, which is consistent with the observed

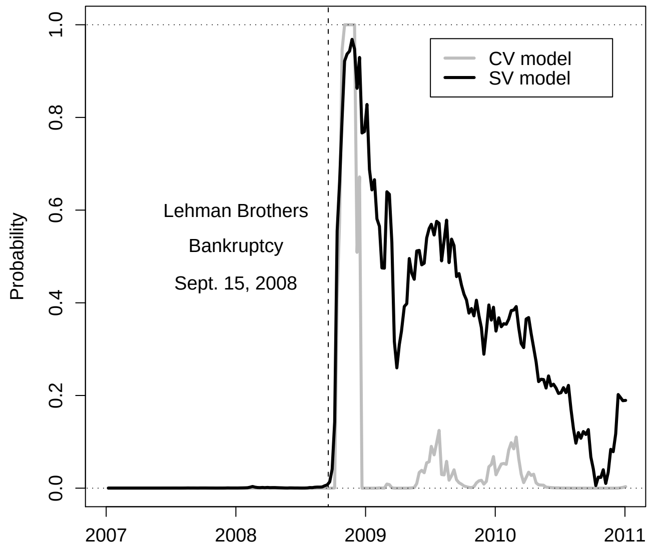

Figure 4: **Estimated One-Year Objective Deflation Probabilities.**
Illustration of the estimated probability of negative net inflation over the following one-year period according to the CV and SV models.

negative year-over-year change in headline CPI observed during these months. The SV model probabilities are markedly higher than the CV model probabilities starting at the end of 2008 through year-end 2010. These higher and more persistent probabilities are partly a reflection of slightly lower short-term expected inflation within the SV model during this period (see Figure 3), but mainly they are due to the SV model's higher conditional volatility estimates that make tail outcomes more likely. Furthermore, in light of the fact that the economy did experience negative headline CPI inflation during 2009, we consider the deflation probability forecasts from the CV model to be low, while the forecasts from the SV model appear more reasonable with estimates in the 30% to 50% range through most of 2009.

4.5 Deflation Protection Option Values

In this section, we use our rolling estimation results to analyze the models' ability to price the deflation protection option embedded in TIPS using the methodology described in Section 2.2. To highlight the difference between the CV and SV models in this regard, Figure 5 shows the two model-implied values of the embedded TIPS deflation protection option measured as the difference in value between a newly issued TIPS and an otherwise identical seasoned TIPS converted into par-coupon yield spreads. The shown series are synthetic, constant five-year par-yield spreads implied by both models. The figure also shows the actually observed yield differences between seasoned and recently issued TIPS with maturities in 2013, 2014, and

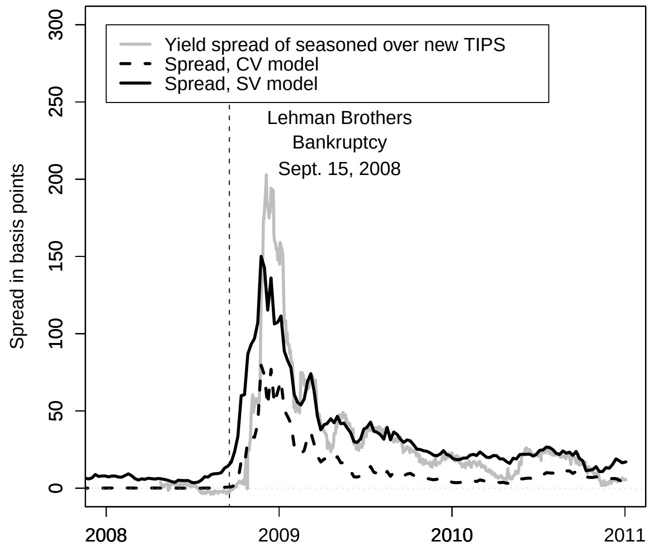

Figure 5: **Five-Year Par-Coupon Yield Spread Between Seasoned and Newly Issued TIPS.**
Illustration of the estimated five-year par-coupon yield spread between a seasoned and a newly issued TIPS according to the CV and SV models. Included is also the spread in yield-to-maturity between comparable pairs of seasoned and newly issued TIPS with approximately five years remaining to maturity as reported by Bloomberg. This series is a proxy for the value of the embedded deflation protection options. See footnote 24 for complete details on the specific nominal and real bond pairs used to generate the series.

2015. At each point in time, we only show the yield spread for the TIPS pair containing the most recently issued five-year TIPS, which we refer to as the *on-the-run* pair, and that represents the closest observable proxy to the model-implied constant-maturity yield spread.[26]

As observed by Christensen et al. (2012), the CV model consistently undervalues the deflation protection option even though it captures its time-variation well. The SV model is much more successful at matching the observed value of the deflation option prior to the crisis, at the peak of the crisis, as well as in the post-crisis period. Table 8 shows that the SV model provides better estimates of the embedded TIPS deflation option over the sample period of April 2008 through December 2010 both in terms of mean fitted error (i.e., -1.50 basis points for the SV model relative to +10.49 basis points for the CV model) and root-mean squared error (i.e., 19.28 versus 25.09 basis points). Looking more carefully at subperiods, both models performed similarly prior to the Lehman bankruptcy in September 2008, but for

[26]Specifically, from April 23, 2008, to April 22, 2009, we use the five-year TIPS with maturity in April 2013 and the ten-year TIPS with maturity in July 2013. From April 23, 2009, to April 23, 2010, we use the five-year TIPS with maturity in April 2014 and the ten-year TIPS with maturity in July 2014. Since April 26, 2010, we use the five-year TIPS with maturity in April 2015 and the ten-year TIPS with maturity in July 2015.

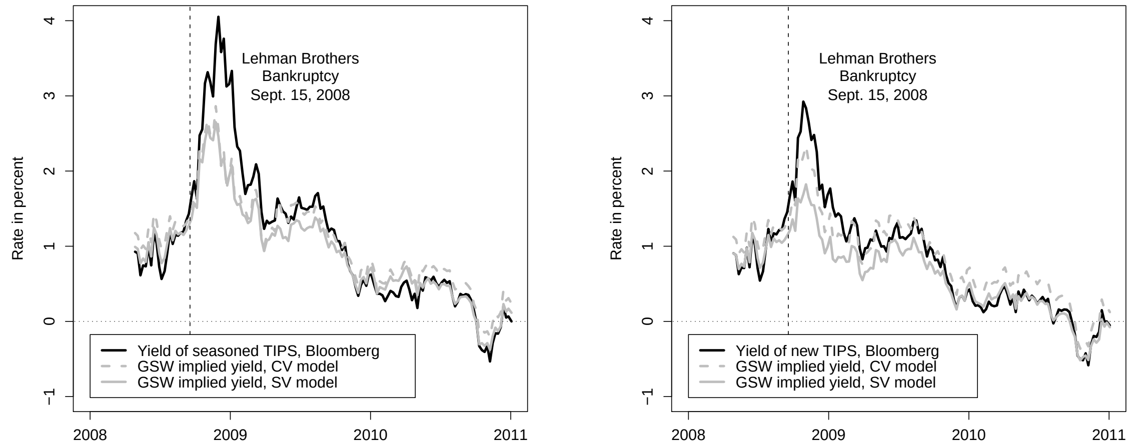

(a) Seasoned TIPS yield.

(b) New TIPS yield.

Figure 6: **Comparison of Model-Implied TIPS Yields to Bloomberg Data.** Comparison of the model-implied yields based on GSW data to the yield-to-maturity of the seasoned and newly issued TIPS as reported by Bloomberg.

the remainder of 2008, the SV model's RMSE was lower at 50.6 basis points as compared to the CV model's value of 62.4 basis points. The SV model again outperformed the CV model over the course of 2009 with an RMSE of 33.4 basis points relative to 40.5 basis points, and in 2010, the corresponding RMSE values were similar at 8.4 versus 7.1 basis points. The ability of the SV model to handle the greater volatility observed during the financial crisis, while performing as well as the CV model before and after the crisis period, is strong evidence in favor of using this model for term structure modeling, especially for interest-rate derivatives pricing and capturing the data's second-moment dynamics.

To further illustrate the relative performance of these two models, we examine the fitted values of the model-implied equivalents of the yield-to-maturity for each of the TIPS in the on-the-run pair separately.[27] For this exercise, we match the timing of the outstanding coupons and principal for each bond exactly, although we neglect the lag in the inflation indexation since such adjustments are typically small for medium-term bonds. Specifically, we generate the net present value of the remaining bond payments using Equation (5) and the fitted real yield curve to convert the bond price into yield-to-maturity. In addition, we add the model-implied value of the deflation protection option before converting the bond price into yield-to-maturity. We explicitly control for the accrued inflation compensation in the option valuation; that is, the option will only be in the money provided that

$$\frac{\Pi_T}{\Pi_t} \leq \frac{1}{\Pi_t/\Pi_0},$$

[27]We are grateful to Kenneth Singleton for suggesting this exercise.

TIPS yield	CV model		SV model	
	Mean	RMSE	Mean	RMSE
(a) Seasoned	1.88	38.68	15.76	39.41
(b) Newly issued	-8.61	23.75	17.26	32.32
Yield spread (a-b)	10.49	25.09	-1.50	19.28
Five-year GSW yield	9.29	28.48	4.67	18.61

Table 8: **Summary Statistics of Pricing Errors for Bloomberg Data.**
The table reports the mean and the root mean squared pricing error of the yield-to-maturity for the seasoned and newly issued TIPS in the pair of TIPS that contains the on-the-run five-year TIPS as reported by Bloomberg. For comparison the last row reports the comparable in-sample mean and root mean squared fitted error of the five-year TIPS yield in the Gürkaynak et al. (2010) data based on the full sample estimation of each model. All numbers are measured in basis points. The data is weekly covering the period from April 25, 2008 to December 31, 2010, a total of 141 observations.

where Π_t/Π_0 is the index ratio as of time t. Thus, the deflation experienced over the remaining life of the bond, Π_T/Π_t, has to negate the accumulated inflation experienced since the bond's issuance.

As shown in Figure 6, both models fit the bond-specific yield data relatively well outside of the peak of the financial crisis in the fall of 2008 and the early part of 2009 when TIPS liquidity was a concern. Table 8 shows that the SV model does not perform as well in pricing the individual bonds as it does in capturing the spread and thus the embedded option values. For the sample period, the SV model has larger mean errors for both the seasoned and newly-issued TIPS. In terms of RMSE, its value for the seasoned bonds is on par with that of the CV model, but it is much higher for the newly-issued bonds. As observed in Table 5 regarding the models' comparative in-sample fit for the nominal and real yield curves, the relative advantage of the SV model is not obvious when examining the data's first moment dynamics, whether for the real yield curve or for individual bond yields. However, the model's ability to price the option values implicit in the spread between the on-the-run bond pairs reflects its advantage in better capturing the data's second moment dynamics. Thus, the introduction of stochastic volatility into term structure models is an important extension for modeling interest rate risk and derivatives pricing.

5 Analysis of the Deflation Risk Premium

In this section, we use regression analysis to identify the determinants of the deflation risk premium defined as the par-bond yield spread between a seasoned and a comparable newly issued TIPS as described in the previous section.[28] Up front, we acknowledge that TIPS mar-

[28]This analysis and the choice of variables are heavily inspired by Christensen and Gillan (2014), who assess the impact on frictions in the TIPS and inflation swap markets from the TIPS purchases included in the Federal Reserve's second program of large-scale asset purchases, frequently referred to a QE2, that operated from November 2010 through June 2011.

ket functioning, along with the functioning of so many other financial markets, was impaired at the peak of the financial crisis, and our models do not readily account for such liquidity effects. As a consequence, we attempt to assess how much of the variation in the deflation risk premium during our sample period reflects outright deflation fears caused by economic uncertainty, and how much could be associated with market illiquidity and limits to arbitrage.

5.1 Econometric Challenge

The correlation between states of the world with near-zero interest rates and states of the world with deflation is intuitively high.[29] Unfortunately, the near-zero interest rates in the U.S. came about as a policy response to the freezing of financial markets. Thus, in the data, poor market functioning coincides with low interest rates. Worse still, in the post-crisis period when financial conditions started to normalize, the reverse pattern was observed; that is, improvement in market functioning goes hand in hand with reduced risk of deflation. Thus, in our regressions, the deflation protection premium, which is our dependent variable, will tend to decline at the same time as measures of market functioning improve without the two having a causal relationship. In short, the results could likely be interpreted as indicating that the yield wedge between seasoned and newly issued TIPS was caused by limits to arbitrage, rather than reflecting true expectations for deflation. This is the ultimate econometric challenge.

5.2 Dependent Variables

We define the deflation risk premium to be the synthetic par-coupon bond yield spread between a seasoned TIPS whose deflation protection option value can be assumed to be zero and a newly issued TIPS where the option is at-the-money. To be consistent with the previous analysis, we limit our focus to the five-year deflation risk premium series. These estimated series from the two models are shown in Figure 7 and represent the dependent variables in our regressions.

5.3 Explanatory Variables

In this section, we provide a brief description of the explanatory variables included in our analysis. While the other factors to be considered are supposed to capture limits to arbitrage or pricing frictions, our first and leading candidate is a measure of priced economic uncertainty, namely the VIX options-implied volatility index. It represents near-term uncertainty about the general stock market as reflected in one-month options on the S&P 500 stock price index and is widely used as a gauge of investor fear and risk aversion. When the price of uncertainty

[29]To see this, invoke the Fisher equation that states that the nominal interest rate equals the real interest rate plus the rate of inflation. If, in addition, deflationary states are low-growth states with low real rates, the high correlation between low nominal interest rates and deflation is reinforced.

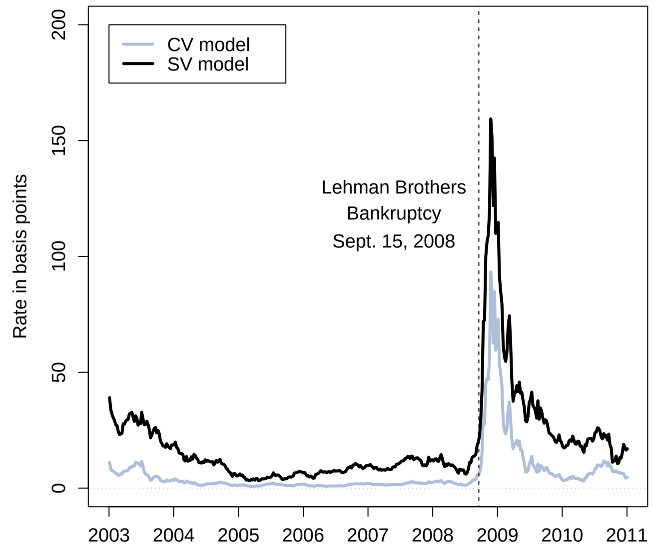

Figure 7: **Five-Year Deflation Risk Premiums.**
Illustration of the estimated five-year deflation risk premiums from the CV and SV models. The data cover the period from January 3, 2003, to December 31, 2010.

goes up as reflected in higher values of the VIX, the value of the TIPS deflation protection option should go up as well.

The second variable is a market illiquidity measure introduced in a recent paper by HPW.[30] They demonstrate that deviations in bond prices in the Treasury securities market from a fitted yield curve represent a measure of noise and illiquidity caused by limited availability of arbitrage capital. Their analysis suggests that the measure is a priced risk factor across several financial markets, which they interpret to imply that their error series represents an economy-wide illiquidity measure that should affect all financial markets including the market for TIPS.

The third variable considered is the yield difference between seasoned, or so-called off-the-run, Treasury securities and the most recently issued, or so-called on-the-run, Treasury security.[31] For each maturity segment in the Treasury bond market, the on-the-run security is typically the most traded security and therefore least penalized in terms of liquidity premiums. For our analysis, the important thing to note is that, provided there is a wide yield spread between liquid on-the-run and comparable seasoned Treasuries, we would expect a similar widening of the yield spread between comparable seasoned and newly issued TIPS.

[30] The data are publicly available at Jun Pan's website: https://sites.google.com/site/junpan2/publications.

[31] We focus on the most widely used ten-year maturity and construct the spread by taking the difference between the off-the-run Treasury par-coupon bond yield from the GSW (2007) database and the on-the-run Treasury par-coupon bond yield from the H.15 series at the Board of Governors.

Our fourth explanatory variable is the excess yield of AAA-rated U.S. industrial corporate bonds over comparable Treasury yields.[32] We note that in choosing the maturity we face a trade off. On one side, we would ideally like to match the maturity of the deflation risk premium measure. However, the credit risk of even AAA-rated industrial bonds cannot be deemed negligible at a five-year horizon. On the other hand, if we focus on very short-term debt where credit risk is entirely negligible, we are far from the desired maturity range. We believe using the two-year credit spread strikes a reasonable balance. As the credit risk component of such highly rated shorter-term bond yields is minimal, the yield spread largely reflect the premium bond investors require for being exposed to the lower trading volume and larger bid-ask spreads in the corporate bond market vis-à-vis the liquid Treasury bond market. Again, if such illiquidity premiums of high-quality corporate bonds are large, we could expect wider yield spreads between comparable seasoned and newly issued TIPS.

The fifth and final variable included is the weekly average of the daily trading volume in the secondary market for TIPS as reported by the Federal Reserve Bank of New York.[33] We use the 8-week moving average to smooth out short-term volatility. This measure should have a negative effect on the deflation risk premium provided it reflects limits to arbitrage as increases in TIPS trading volume should, in most cases, reduce mispricing.

5.4 Regression Results

Table 9 reports the results of regressing the five-year deflation risk premium measure from the CV (top panel) and SV (bottom panel) models on the explanatory variables described in the previous section.[34]

First, the regressions with the deflation risk premium measure from the SV model always produce higher adjusted R^2s than the regressions based on the deflation risk premium implied by the CV model. Second, based on the measure from the SV model, the adjusted R^2 easily exceeds 80%. Thus, in general, we feel that our five explanatory variables are successful in capturing the variation in the deflation risk premium. Third, and most importantly, the VIX is always a highly significant explanatory variable with an estimated coefficient of the right sign and of economically meaningful size. Thus, one robust finding is that financial market uncertainty as measured by the VIX is a key determinant of the deflation risk premium as represented by the at-the-money deflation protection option values implied by the CV and SV models. Furthermore, and not surprisingly, the measure of financial market illiquidity introduced by HPW also consistently has a high explanatory power with a positive sign for its estimated coefficient. This suggests that at least part of the variation in our deflation risk premium measure reflects financial market illiquidity. In addition, the other three measures of market liquidity and market functioning, the off-the-run yield spread, the AAA credit spread,

[32] The data are from Bloomberg; See Christensen et al. (2014b) for details.
[33] The data are available at: http://www.newyorkfed.org/markets/statrel.html.
[34] The results reported in Table 9 are robust to using other maturities and sample periods.

Explanatory Variables	CV model							
	(1)	(2)	(3)	(4)	(5)	(6)	(7)	(8)
Constant	-0.12	-0.05**	-0.08**	-0.03**	0.13**	-0.07**	-0.04**	-0.04**
	(-15.41)	(-11.60)	(-12.37)	(-4.41)	(6.17)	(-10.18)	(-2.85)	(-2.72)
VIX	0.89**					0.20**	0.17**	0.26**
	(26.46)					(3.86)	(3.11)	(4.54)
HPW measure		0.03**				0.03**	0.03**	0.04**
		(35.75)				(15.41)	(15.84)	(12.71)
Off-The-Run Spread			0.87**					-0.19**
			(26.93)					(-2.62)
AAA Credit Spread				0.21**				-0.06**
				(18.41)				(-3.67)
TIPS Trading Volume					-0.01**		-0.00**	-0.00
					(-3.12)		(-2.99)	(-1.37)
Adjusted R^2	0.63	0.75	0.63	0.45	0.02	0.76	0.77	0.77

Explanatory Variables	SV model							
	(1)	(2)	(3)	(4)	(5)	(6)	(7)	(8)
Constant	-0.17**	-0.01	-0.09**	0.03*	0.39**	-0.10**	0.05*	0.00
	(-13.37)	(-1.91)	(-9.01)	(2.42)	(10.95)	(-8.24)	(2.47)	(-0.04)
VIX	1.74**					0.77**	0.61**	0.67**
	(32.41)					(8.75)	(7.29)	(7.41)
HPW measure		0.06**				0.04**	0.04**	0.04**
		(36.11)				(12.72)	(14.91)	(10.17)
Off-The-Run Spread			1.72**					0.10
			(34.60)					(0.82)
AAA Credit Spread				0.36**				-0.10**
				(17.01)				(-3.88)
TIPS Trading Volume					-0.03**		-0.02**	-0.01**
					(-5.79)		(-8.39)	(-4.03)
Adjusted R^2	0.72	0.76	0.74	0.41	0.07	0.79	0.82	0.83

Table 9: **Deflation Risk Premium Regression Results 2003-2010.**
The top panel reports the results of regressions with the par-bond yield spread between a seasoned and a newly issued five-year TIPS implied by the CV model, while the bottom panel reports the regression results for the corresponding measure implied by the SV model. T-statistics are reported in parentheses. Asterisks * and ** indicate significance at the 5 percent and 1 percent levels, respectively. The data sample is weekly covering the period from January 3, 2003, to December 31, 2010, a total of 418 observations.

and the TIPS trading volume, all individually have the expected sign, but once we combine them with the VIX and the HPW measure, their added explanatory power is low and their estimated coefficients tend to switch sign or lose statistical significance. This suggests that they are secondary in determining the deflation risk premium once we have controlled for the variation in the VIX and the HPW measure. Since we have not corrected the TIPS yields used in model estimation for any liquidity effects, these results were to be expected. Still, we consider the high significance of the VIX in these regressions a strong indication that the model-implied deflation protection option values are real and not a spurious artefact caused by changes in TIPS market liquidity.

6 Conclusion

In this paper, we examine the deflation protection option embedded in TIPS over the period from 2003 to 2010, including the depths of the financial crisis in late 2008 and early 2009. To do so, we modify the joint model of nominal and real bond yields introduced in CLR by replacing its constant volatility (CV) assumption with stochastic volatility (SV) driven by the model's nominal and real level factors. Our preferred specification of the SV model delivers reasonable decompositions of breakeven inflation (i.e., the spread between nominal and real Treasury yields) into expected inflation and inflation risk premiums, showing that this model captures the data's first moment dynamics as well as the CV model. However, the SV model is shown to be better able to price the value of deflation protection embedded in TIPS and proxied for here by the difference between similar TIPS with differing degrees of accumulated inflation protection. This result highlights that the SV model is better able to capture the volatility dynamics observed in the data and critical to derivatives pricing. Based on this evidence, the proposed SV model should be useful for judging bond investors' views on the tail risk of deflation as well as their inflation expectations. The SV model is an obvious candidate for pricing derivative products in the inflation swap market, a topic we leave for future research.

In analyzing the deflation risk premium defined as the par-bond yield spread between a seasoned and a comparable newly issued TIPS, our results suggest that a significant part of the variation in the deflation risk premium is associated with general economic uncertainty. Still, a notable part of the variation is associated with measures of market illiquidity. Thus, correcting TIPS yields for liquidity effects would be desirable (see Pflueger and Viceira 2013 and D'Amico et al. 2014 for examples), but this is another topic that we leave for future research.

Finally, we end our sample in 2010 to avoid addressing the problem of the zero lower bound of nominal yields. However, going forward, this will be a critical issue to address as short-term U.S. Treasury yields have been near the zero lower bound since mid-2011. Christensen and Rudebusch (2014) introduce a tractable shadow-rate AFNS model class, which respects the zero lower bound for nominal bond yields and could be explored further. Again, we leave this important endeavor for future research.

Appendices

A). **Bond Price Formulas**

In the SV model, nominal zero-coupon bond prices are given by

$$P^N(t,T) = E_t^Q\big[\exp\big(-\int_t^T r_u^N du\big)\big] = \exp\big(B_1^N(t,T)L_t^N + B_2^N(t,T)S_t + B_3^N(t,T)C_t + B_4^N(t,T)L_t^R + A^N(t,T)\big),$$

where $B_1^N(t,T)$, $B_2^N(t,T)$, $B_3^N(t,T)$, and $B_4^N(t,T)$ are the unique solutions to the following system of ODEs

$$\begin{pmatrix} \frac{dB_1^N(t,T)}{dt} \\ \frac{dB_2^N(t,T)}{dt} \\ \frac{dB_3^N(t,T)}{dt} \\ \frac{dB_4^N(t,T)}{dt} \end{pmatrix} = \begin{pmatrix} 1 \\ 1 \\ 0 \\ 0 \end{pmatrix} + \begin{pmatrix} \kappa_{L^N}^Q & 0 & 0 & 0 \\ 0 & \lambda & 0 & 0 \\ 0 & -\lambda & \lambda & 0 \\ 0 & 0 & 0 & \kappa_{L^R}^Q \end{pmatrix} \begin{pmatrix} B_1^N(t,T) \\ B_2^N(t,T) \\ B_3^N(t,T) \\ B_4^N(t,T) \end{pmatrix}$$

$$-\frac{1}{2}\sum_{j=1}^4 \left[\begin{pmatrix} \sigma_{11} & 0 & 0 & 0 \\ 0 & \sigma_{22} & 0 & 0 \\ 0 & 0 & \sigma_{33} & 0 \\ 0 & 0 & 0 & \sigma_{44} \end{pmatrix} \begin{pmatrix} (B_1^N)^2 & B_1^N B_2^N & B_1^N B_3^N & B_1^N B_4^N \\ B_1^N B_2^N & (B_2^N)^2 & B_2^N B_3^N & B_2^N B_4^N \\ B_1^N B_3^N & B_2^N B_3^N & (B_3^N)^2 & B_3^N B_4^N \\ B_1^N B_4^N & B_2^N B_4^N & B_3^N B_4^N & (B_4^N)^2 \end{pmatrix} \begin{pmatrix} \sigma_{11} & 0 & 0 & 0 \\ 0 & \sigma_{22} & 0 & 0 \\ 0 & 0 & \sigma_{33} & 0 \\ 0 & 0 & 0 & \sigma_{44} \end{pmatrix} \right]_{j,j} (\delta^j)',$$

and γ and δ are given by

$$\gamma = \begin{pmatrix} 0 \\ 1 \\ 1 \\ 0 \end{pmatrix} \quad \text{and} \quad \delta = \begin{pmatrix} 1 & 0 & 0 & 0 \\ 0 & 0 & 0 & 0 \\ 0 & 0 & 0 & 0 \\ 0 & 0 & 0 & 1 \end{pmatrix}.$$

This structure implies that the factor loadings in the nominal zero-coupon bond price function are given by the unique solution to the following set of ODEs

$$\begin{aligned}
\frac{dB_1^N(t,T)}{dt} &= 1 + \kappa_{L^N}^Q B_1^N(t,T) - \frac{1}{2}\sigma_{11}^2 B_1^N(t,T)^2, \quad B_1^N(T,T) = \overline{B}_1^N, \\
\frac{dB_2^N(t,T)}{dt} &= 1 + \lambda B_2^N(t,T), \quad B_2^N(T,T) = \overline{B}_2^N, \\
\frac{dB_3^N(t,T)}{dt} &= -\lambda B_2^N(t,T) + \lambda B_3^N(t,T), \quad B_3^N(T,T) = \overline{B}_3^N, \\
\frac{dB_4^N(t,T)}{dt} &= \kappa_{L^R}^Q B_4^N(t,T) - \frac{1}{2}\sigma_{44}^2 B_4^N(t,T)^2, \quad B_4^N(T,T) = \overline{B}_4^N.
\end{aligned}$$

These four ODEs have the following unique solution[35]

$$\begin{aligned}
B_1^N(t,T) &= \frac{-2[e^{\phi^N(T-t)}-1] + \overline{B}_1^N e^{\phi^N(T-t)}(\phi^N - \kappa_{L^N}^Q) + \overline{B}_1^N(\phi^N + \kappa_{L^N}^Q)}{2\phi^N + (\phi^N + \kappa_{L^N}^Q - \overline{B}_1^N\sigma_{11}^2)[e^{\phi^N(T-t)}-1]}, \\
B_2^N(t,T) &= e^{-\lambda(T-t)}\overline{B}_2^N - \frac{1-e^{-\lambda(T-t)}}{\lambda}, \\
B_3^N(t,T) &= \lambda(T-t)e^{-\lambda(T-t)}\overline{B}_2^N + \overline{B}_3^N e^{-\lambda(T-t)} + \Big[(T-t)e^{-\lambda(T-t)} - \frac{1-e^{-\lambda(T-t)}}{\lambda}\Big], \\
B_4^N(t,T) &= \frac{2\kappa_{L^R}^Q \overline{B}_4^N}{(2\kappa_{L^R}^Q - \overline{B}_4^N\sigma_{44}^2)e^{\kappa_{L^R}^Q(T-t)} + \overline{B}_4^N\sigma_{44}^2},
\end{aligned}$$

where

$$\phi^N = \sqrt{(\kappa_{L^N}^Q)^2 + 2\sigma_{11}^2}.$$

Now, the $A^N(t,T)$-function in the yield-adjustment term in the nominal zero-coupon bond yield function

[35] The calculations leading to this result are available upon request.

is given by the solution to the following ODE

$$\frac{dA^N(t,T)}{dt} = -B^N(t,T)'K^Q\theta^Q - \frac{1}{2}\sigma_2^2 B_2^N(t,T)^2 - \frac{1}{2}\sigma_3^2 B_3^N(t,T)^2, \quad A^N(T,T) = \overline{A}^N.$$

This ODE has the following unique solution

$$\begin{aligned}
A^N(t,T) &= \overline{A}^N + \frac{2\kappa_{L^N}^Q \theta_{L^N}^Q}{\sigma_{11}^2} \ln\Big[\frac{2\phi^N e^{\frac{1}{2}(\phi^N+\kappa_{L^N}^Q)(T-t)}}{2\phi^N + (\phi^N + \kappa_{L^N}^Q - \overline{B}_1^N \sigma_{11}^2)(e^{\phi^N(T-t)}-1)}\Big] \\
&+\sigma_{22}^2\Big[\frac{1}{2\lambda^2}(T-t) - \frac{(1+\lambda\overline{B}_2^N)}{\lambda^3}[1-e^{-\lambda(T-t)}] + \frac{(1+\lambda\overline{B}_2^N)^2}{4\lambda^3}[1-e^{-2\lambda(T-t)}]\Big] \\
&+\sigma_{33}^2\Big[\frac{1}{2\lambda^2}(T-t) + \frac{1+\lambda\overline{B}_2^N}{\lambda^2}(T-t)e^{-\lambda(T-t)} - \frac{(1+\lambda\overline{B}_2^N)^2}{4\lambda}(T-t)^2 e^{-2\lambda(T-t)} \\
&\quad - \frac{(1+\lambda\overline{B}_2^N)(3+\lambda\overline{B}_2^N + 2\lambda\overline{B}_3^N)}{4\lambda^2}(T-t)e^{-2\lambda(T-t)} \\
&\quad + \frac{(2+\lambda\overline{B}_2^N + \lambda\overline{B}_3^N)^2 + (1+\lambda\overline{B}_3^N)^2}{8\lambda^3}[1-e^{-2\lambda(T-t)}] - \frac{2+\lambda\overline{B}_2^N + \lambda\overline{B}_3^N}{\lambda^3}[1-e^{-\lambda(T-t)}]\Big] \\
&+\frac{2\kappa_{L^R}^Q \theta_{L^R}^Q}{\sigma_{44}^2} \ln\Big[\frac{2\kappa_{L^R}^Q e^{\kappa_{L^R}^Q(T-t)}}{(2\kappa_{L^R}^Q - \overline{B}_4^N \sigma_{44}^2)e^{\kappa_{L^R}^Q(T-t)} + \overline{B}_4^N \sigma_{44}^2}\Big].
\end{aligned}$$

In the SV model, the real zero-coupon bond prices are given by

$$P^R(t,T) = E_t^Q\big[\exp\big(-\int_t^T r_u^R du\big)\big] = \exp\big(B_1^R(t,T)L_t^N + B_2^R(t,T)S_t + B_3^R(t,T)C_t + B_4^R(t,T)L_t^R + A^R(t,T)\big),$$

where $B_1^R(t,T)$, $B_2^R(t,T)$, $B_3^R(t,T)$, and $B_4^R(t,T)$ are the unique solutions to the following system of ODEs

$$\begin{pmatrix} \frac{dB_1^R(t,T)}{dt} \\ \frac{dB_2^R(t,T)}{dt} \\ \frac{dB_3^R(t,T)}{dt} \\ \frac{dB_4^R(t,T)}{dt} \end{pmatrix} = \begin{pmatrix} 0 \\ \alpha^R \\ 0 \\ 1 \end{pmatrix} + \begin{pmatrix} \kappa_{L^N}^Q & 0 & 0 & 0 \\ 0 & \lambda & 0 & 0 \\ 0 & -\lambda & \lambda & 0 \\ 0 & 0 & 0 & \kappa_{L^R}^Q \end{pmatrix} \begin{pmatrix} B_1^R(t,T) \\ B_2^R(t,T) \\ B_3^R(t,T) \\ B_4^R(t,T) \end{pmatrix}$$

$$-\frac{1}{2}\sum_{j=1}^{4}\left[\begin{pmatrix} \sigma_{11} & 0 & 0 & 0 \\ 0 & \sigma_{22} & 0 & 0 \\ 0 & 0 & \sigma_{33} & 0 \\ 0 & 0 & 0 & \sigma_{44} \end{pmatrix}\begin{pmatrix} (B_1^R)^2 & B_1^R B_2^R & B_1^R B_3^R & B_1^R B_4^R \\ B_1^R B_2^R & (B_2^R)^2 & B_2^R B_3^R & B_2^R B_4^R \\ B_1^R B_3^R & B_2^R B_3^R & (B_3^R)^2 & B_3^R B_4^R \\ B_1^R B_4^R & B_2^R B_4^R & B_3^R B_4^R & (B_4^R)^2 \end{pmatrix}\begin{pmatrix} \sigma_{11} & 0 & 0 & 0 \\ 0 & \sigma_{22} & 0 & 0 \\ 0 & 0 & \sigma_{33} & 0 \\ 0 & 0 & 0 & \sigma_{44} \end{pmatrix}\right]_{j,j} (\delta^j)'.$$

This implies that the factor loadings in the real zero-coupon bond price function are given by the unique solution to the following set of ODEs

$$\begin{aligned}
\frac{dB_1^R(t,T)}{dt} &= \kappa_{L^N}^Q B_1^R(t,T) - \frac{1}{2}\sigma_{11}^2 B_1^R(t,T)^2, \quad B_1^R(T,T) = \overline{B}_1^R, \\
\frac{dB_2^R(t,T)}{dt} &= \alpha^R + \lambda B_2^R(t,T), \quad B_2^R(T,T) = \overline{B}_2^R, \\
\frac{dB_3^R(t,T)}{dt} &= -\lambda B_2^R(t,T) + \lambda B_3^R(t,T), \quad B_3^R(T,T) = \overline{B}_3^R, \\
\frac{dB_4^R(t,T)}{dt} &= 1 + \kappa_{L^R}^Q B_4^R(t,T) - \frac{1}{2}\sigma_{44}^2 B_4^R(t,T)^2, \quad B_4^R(T,T) = \overline{B}_4^R.
\end{aligned}$$

These four ODEs have the following unique solution[36]

$$
\begin{aligned}
B_1^R(t,T) &= \frac{2\kappa_{LN}^Q \overline{B}_1^R}{(2\kappa_{LN}^Q - \overline{B}_1^R\sigma_{11}^2)e^{\kappa_{LN}^Q(T-t)} + \overline{B}_1^R\sigma_{11}^2}, \\
B_2^R(t,T) &= e^{-\lambda(T-t)}\overline{B}_2^R - \alpha^R \frac{1-e^{-\lambda(T-t)}}{\lambda}, \\
B_3^R(t,T) &= \lambda(T-t)e^{-\lambda(T-t)}\overline{B}_2^R + \overline{B}_3^R e^{-\lambda(T-t)} + \alpha^R\Big[(T-t)e^{-\lambda(T-t)} - \frac{1-e^{-\lambda(T-t)}}{\lambda}\Big], \\
B_4^R(t,T) &= \frac{-2[e^{\phi^R(T-t)}-1] + \overline{B}_4^R e^{\phi^R(T-t)}(\phi^R - \kappa_{LR}^Q) + \overline{B}_4^R(\phi^R + \kappa_{LR}^Q)}{2\phi^R + (\phi^R + \kappa_{LR}^Q - \overline{B}_4^R\sigma_{44}^2)[e^{\phi^R(T-t)}-1]},
\end{aligned}
$$

where

$$\phi^R = \sqrt{(\kappa_{LR}^Q)^2 + 2\sigma_{44}^2}.$$

The $A^R(t,T)$-function in the yield-adjustment term in the real zero-coupon bond yield function is given by the solution to the following ODE

$$\frac{dA^R(t,T)}{dt} = -B^R(t,T)'K^Q\theta^Q - \frac{1}{2}\sigma_2^2 B_2^R(t,T)^2 - \frac{1}{2}\sigma_3^2 B_3^R(t,T)^2, \quad A^R(T,T) = \overline{A}^R,$$

which is

$$
\begin{aligned}
A^R(t,T) = {} & \overline{A}^R + \frac{2\kappa_{LN}^Q\theta_{LN}^Q}{\sigma_{11}^2}\ln\left[\frac{2\kappa_{LN}^Q e^{\kappa_{LN}^Q(T-t)}}{(2\kappa_{LN}^Q - \overline{B}_1^R\sigma_{11}^2)e^{\kappa_{LN}^Q(T-t)} + \overline{B}_1^R\sigma_{11}^2}\right] \\
& + \sigma_{22}^2\Big[\frac{(\alpha^R)^2}{2\lambda^2}(T-t) - \alpha^R\frac{(\alpha^R + \lambda\overline{B}_2^R)}{\lambda^3}[1-e^{-\lambda(T-t)}] + \frac{(\alpha^R + \lambda\overline{B}_2^R)^2}{4\lambda^3}[1-e^{-2\lambda(T-t)}]\Big] \\
& + \sigma_{33}^2\Bigg[\frac{(\alpha^R)^2}{2\lambda^2}(T-t) + \alpha^R\frac{\alpha^R + \lambda\overline{B}_2^R}{\lambda^2}(T-t)e^{-\lambda(T-t)} - \frac{(\alpha^R + \lambda\overline{B}_2^R)^2}{4\lambda}(T-t)^2e^{-2\lambda(T-t)} \\
& \quad - \frac{(\alpha^R + \lambda\overline{B}_2^R)(3\alpha^R + \lambda\overline{B}_2^R + 2\lambda\overline{B}_3^R)}{4\lambda^2}(T-t)e^{-2\lambda(T-t)} \\
& \quad + \frac{(2\alpha^R + \lambda\overline{B}_2^R + \lambda\overline{B}_3^R)^2 + (\alpha^R + \lambda\overline{B}_3^R)^2}{8\lambda^3}[1-e^{-2\lambda(T-t)}] \\
& \quad - \alpha^R\frac{2\alpha^R + \lambda\overline{B}_2^R + \lambda\overline{B}_3^R}{\lambda^3}[1-e^{-\lambda(T-t)}]\Bigg] \\
& + \frac{2\kappa_{LR}^Q\theta_{LR}^Q}{\sigma_{44}^2}\ln\left[\frac{2\phi^R e^{\frac{1}{2}(\phi^R + \kappa_{LR}^Q)(T-t)}}{2\phi^R + (\phi^R + \kappa_{LR}^Q - \overline{B}_4^R\sigma_{44}^2)(e^{\phi^R(T-t)}-1)}\right].
\end{aligned}
$$

B). Calculation of the NPV of the TIPS Principal Deflation Protection

In general, we are interested in finding the NPV of terminal payoffs from TIPS contingent on the cumulated inflation being below some critical value q, specifically the following difference is of interest

$$E_t^Q\left[e^{-\int_t^T r_s^N ds}\mathbf{1}_{\{\frac{\Pi_T}{\Pi_t}\leq 1+q\}}\right] - E_t^Q\left[e^{-\int_t^T r_s^R ds}\mathbf{1}_{\{\frac{\Pi_T}{\Pi_t}\leq 1+q\}}\right].$$

Thus, the states of the world of interest are characterized by

$$\frac{\Pi_T}{\Pi_t} \leq 1+q \iff Y_{t,T} = \int_t^T (r_s^N - r_s^R)ds \leq \ln(1+q).$$

[36]The calculations leading to this result are available upon request.

Since we are pricing, we need the dynamics of the state variables under the Q-measure

$$\begin{pmatrix} dL_t^N \\ dS_t \\ dC_t \\ dL_t^R \\ dY_{0,t} \end{pmatrix} = \begin{pmatrix} \kappa_{L^N}^Q & 0 & 0 & 0 & 0 \\ 0 & \lambda & -\lambda & 0 & 0 \\ 0 & 0 & \lambda & 0 & 0 \\ 0 & 0 & 0 & \kappa_{L^R}^Q & 0 \\ -1 & -(1-\alpha^R) & 0 & 1 & 0 \end{pmatrix} \left[\begin{pmatrix} \theta_{L^N}^Q \\ 0 \\ 0 \\ \theta_{L^R}^Q \\ 0 \end{pmatrix} - \begin{pmatrix} L_t^N \\ S_t \\ C_t \\ L_t^R \\ Y_{0,t} \end{pmatrix} \right] dt$$
$$+ \begin{pmatrix} \sigma_{11} & 0 & 0 & 0 & 0 \\ 0 & \sigma_{22} & 0 & 0 & 0 \\ 0 & 0 & \sigma_{33} & 0 & 0 \\ 0 & 0 & 0 & \sigma_{44} & 0 \\ 0 & 0 & 0 & 0 & 0 \end{pmatrix} \begin{pmatrix} \sqrt{L_t^N} & 0 & 0 & 0 & 0 \\ 0 & \sqrt{1} & 0 & 0 & 0 \\ 0 & 0 & \sqrt{1} & 0 & 0 \\ 0 & 0 & 0 & \sqrt{L_t^R} & 0 \\ 0 & 0 & 0 & 0 & \sqrt{1} \end{pmatrix} \begin{pmatrix} dW_t^{L^N,Q} \\ dW_t^{S,Q} \\ dW_t^{C,Q} \\ dW_t^{L^R,Q} \\ dW_t^{Y,Q} \end{pmatrix},$$

where $Z_{0,t} = (L_t^N, S_t, C_t, L_t^R, Y_{0,t})$ represents the augmented state vector.

Now, define the following two intermediate functions

$$\psi^1(\overline{B}, t, T) = E_t^Q\left[e^{-\int_t^T r_s^R ds} e^{\overline{B}' Z_{t,T}}\right] \quad \text{and} \quad \psi^2(\overline{B}, t, T) = E_t^Q\left[e^{-\int_t^T r_s^N ds} e^{\overline{B}' Z_{t,T}}\right].$$

In order to calculate $\psi^1(\overline{B}, t, T)$ and $\psi^2(\overline{B}, t, T)$, we summarize the Q-dynamics by the following matrices and vectors

$$K^Q = \begin{pmatrix} \kappa_{L^N}^Q & 0 & 0 & 0 & 0 \\ 0 & \lambda & -\lambda & 0 & 0 \\ 0 & 0 & \lambda & 0 & 0 \\ 0 & 0 & 0 & \kappa_{L^R}^Q & 0 \\ -1 & -(1-\alpha^R) & 0 & 1 & 0 \end{pmatrix}, \quad \theta^Q = \begin{pmatrix} \theta_{L^N}^Q \\ 0 \\ 0 \\ \theta_{L^R}^Q \\ 0 \end{pmatrix}, \quad \Sigma = \begin{pmatrix} \sigma_{11} & 0 & 0 & 0 & 0 \\ 0 & \sigma_{22} & 0 & 0 & 0 \\ 0 & 0 & \sigma_{33} & 0 & 0 \\ 0 & 0 & 0 & \sigma_{44} & 0 \\ 0 & 0 & 0 & 0 & 0 \end{pmatrix},$$

$$\rho^N = \begin{pmatrix} 1 \\ 1 \\ 0 \\ 0 \\ 0 \end{pmatrix}, \quad \rho^R = \begin{pmatrix} 0 \\ \alpha^R \\ 0 \\ 1 \\ 0 \end{pmatrix}.$$

Furthermore, γ and δ are given by

$$\gamma = \begin{pmatrix} 0 \\ 1 \\ 1 \\ 0 \\ 1 \end{pmatrix} \quad \text{and} \quad \delta = \begin{pmatrix} 1 & 0 & 0 & 0 & 0 \\ 0 & 0 & 0 & 0 & 0 \\ 0 & 0 & 0 & 0 & 0 \\ 0 & 0 & 0 & 1 & 0 \\ 0 & 0 & 0 & 0 & 0 \end{pmatrix}.$$

From Duffie, Pan, and Singleton (2000) it follows that

$$\psi^1(\overline{B}, t, T) = \exp(B_{\psi^1}(t,T)' Z_{t,t} + A_{\psi^1}(t,T)),$$

where $B_{\psi^1}(t,T)$ and $A_{\psi^1}(t,T)$ are the solutions to the following system of ODEs

$$\frac{dB_{\psi^1}(t,T)}{dt} = \rho^R + (K^Q)' B_{\psi^1}(t,T) - \frac{1}{2}\sum_{j=1}^{5} (\Sigma' B_{\psi^1}(t,T) B_{\psi^1}(t,T)' \Sigma)_{j,j} (\delta^j)', \quad B_{\psi^1}(T,T) = \overline{B}, \tag{19}$$

$$\frac{dA_{\psi^1}(t,T)}{dt} = -B_{\psi^1}(t,T)' K^Q \theta^Q - \frac{1}{2}\sum_{j=1}^{5} (\Sigma' B_{\psi^1}(t,T) B_{\psi^1}(t,T)' \Sigma)_{j,j} \gamma^j, \quad A_{\psi^1}(T,T) = 0. \tag{20}$$

This system of ODEs can be solved analytically and the solution is provided in the following proposition.

Proposition 1:

Let the state variables be given by $Z_{t,T} = (L_t^N, S_t, C_t, L_t^R, Y_{t,T})$, and let the real instantaneous risk-free rate be given by

$$r_t^R = (\rho^R)' X_t,$$

then

$$\psi^1(\overline{B}, t, T) = \exp(B_{\psi^1}^1(t,T)L_t^N + B_{\psi^1}^2(t,T)S_t + B_{\psi^1}^3(t,T)C_t + B_{\psi^1}^4(t,T)L_t^R + B_{\psi^1}^5(t,T)Y_{t,t} + A_{\psi^1}(t,T))$$

where[37]

$$\begin{aligned}
B_{\psi^1}^1(t,T) &= \frac{-2\rho_1[e^{\phi_{\psi^1}^N(T-t)} - 1] + \overline{B}^1(\phi_{\psi^1}^N - \kappa_{L^N}^Q)e^{\phi_{\psi^1}^N(T-t)} + \overline{B}^1(\phi_{\psi^1}^N + \kappa_{L^N}^Q)}{2\phi_{\psi^1}^N + (\phi_{\psi^1}^N + \kappa_{L^N}^Q - \overline{B}^1\sigma_{11}^2)[e^{\phi_{\psi^1}^N(T-t)} - 1]}, \\
B_{\psi^1}^2(t,T) &= e^{-\lambda(T-t)}\overline{B}^2 - [\alpha^R - (1-\alpha^R)\overline{B}^5]\frac{1-e^{-\lambda(T-t)}}{\lambda}, \\
B_{\psi^1}^3(t,T) &= e^{-\lambda(T-t)}\overline{B}^3 + \lambda(T-t)e^{-\lambda(T-t)}\overline{B}^2 + [\alpha^R - (1-\alpha^R)\overline{B}^5]\Big\{(T-t)e^{-\lambda(T-t)} - \frac{1-e^{-\lambda(T-t)}}{\lambda}\Big\}, \\
B_{\psi^1}^4(t,T) &= \frac{-2\rho_4[e^{\phi_{\psi^1}^R(T-t)} - 1] + \overline{B}^4(\phi_{\psi^1}^R - \kappa_{L^R}^Q)e^{\phi_{\psi^1}^R(T-t)} + \overline{B}^4(\phi_{\psi^1}^R + \kappa_{L^R}^Q)}{2\phi_{\psi^1}^R + (\phi_{\psi^1}^R + \kappa_{L^R}^Q - \overline{B}^4\sigma_{44}^2)[e^{\phi_{\psi^1}^R(T-t)} - 1]}, \\
B_{\psi^1}^5(t,T) &= \overline{B}^5,
\end{aligned}$$

and

$$\begin{aligned}
A_{\psi^1}(t,T) = {} & \frac{2\kappa_{L^N}^Q\theta_{L^N}^Q}{\sigma_{11}^2}\ln\left[\frac{2\phi_{\psi^1}^N e^{\frac{1}{2}(\phi_{\psi^1}^N + \kappa_{L^N}^Q)(T-t)}}{2\phi_{\psi^1}^N + (\phi_{\psi^1}^N + \kappa_{L^N}^Q - \overline{B}^1\sigma_{11}^2)[e^{\phi_{\psi^1}^N(T-t)} - 1]}\right] \\
& + \sigma_{22}^2[\alpha^R - (1-\alpha^R)\overline{B}^5 + \lambda\overline{B}^2]^2\frac{1-e^{-2\lambda(T-t)}}{4\lambda^3} + \frac{\sigma_2^2}{2}\frac{[\alpha^R - (1-\alpha^R)\overline{B}^5]^2}{\lambda^2}(T-t) \\
& - \sigma_{22}^2[\alpha^R - (1-\alpha^R)\overline{B}^5 + \lambda\overline{B}^2][\alpha^R - (1-\alpha^R)\overline{B}^5]\frac{1-e^{-\lambda(T-t)}}{\lambda^3} \\
& + \sigma_{33}^2[\alpha^R - (1-\alpha^R)\overline{B}^5 + \lambda\overline{B}^3]^2\frac{1-e^{-2\lambda(T-t)}}{4\lambda^3} + \frac{\sigma_{33}^2}{2}\frac{[\alpha^R - (1-\alpha^R)\overline{B}^5]^2}{\lambda^2}(T-t) \\
& + \frac{\sigma_{33}^2}{2}[\alpha^R - (1-\alpha^R)\overline{B}^5 + \lambda\overline{B}^2]^2\Big[-\frac{1}{2\lambda}(T-t)^2e^{-2\lambda(T-t)} - \frac{1}{2\lambda^2}(T-t)e^{-2\lambda(T-t)} + \frac{1-e^{-2\lambda(t-t)}}{4\lambda^3}\Big] \\
& - \sigma_{33}^2[\alpha^R - (1-\alpha^R)\overline{B}^5 + \lambda\overline{B}^3][\alpha^R - (1-\alpha^R)\overline{B}^5]\frac{1-e^{-\lambda(T-t)}}{\lambda^3} \\
& + \sigma_{33}^2\frac{[\alpha^R - (1-\alpha^R)\overline{B}^5 + \lambda\overline{B}^3][\alpha^R - (1-\alpha^R)\overline{B}^5 + \lambda\overline{B}^2]}{\lambda}\Big[-\frac{1}{2\lambda}(T-t)e^{-2\lambda(T-t)} + \frac{1-e^{-2\lambda(T-t)}}{4\lambda^2}\Big] \\
& - \sigma_{33}^2\frac{[\alpha^R - (1-\alpha^R)\overline{B}^5][\alpha^R - (1-\alpha^R)\overline{B}^5 + \lambda\overline{B}^2]}{\lambda}\Big[-\frac{1}{\lambda}(T-t)e^{-\lambda(T-t)} + \frac{1-e^{-\lambda(T-t)}}{\lambda^2}\Big] \\
& + \frac{2\kappa_{L^R}^Q\theta_{L^R}^Q}{\sigma_{44}^2}\ln\left[\frac{2\phi_{\psi^1}^R e^{\frac{1}{2}(\phi_{\psi^1}^R + \kappa_{L^R}^Q)(T-t)}}{2\phi_{\psi^1}^R + (\phi_{\psi^1}^R + \kappa_{L^R}^Q - \overline{B}^4\sigma_{44}^2)[e^{\phi_{\psi^1}^R(T-t)} - 1]}\right]
\end{aligned}$$

with

$$\phi_{\psi^1}^N = \sqrt{(\kappa_{L^N}^Q)^2 + 2\rho_1\sigma_{11}^2}, \quad \rho_1 = -\overline{B}^5, \quad \phi_{\psi^1}^R = \sqrt{(\kappa_{L^R}^Q)^2 + 2\rho_4\sigma_{44}^2}, \quad \text{and} \quad \rho_4 = 1 + \overline{B}^5.$$

[37]The calculations leading to this result are available upon request.

Using a similar approach, it holds that

$$\psi^2(\overline{B}, t, T) = \exp(B_{\psi^2}(t,T)' Z_{t,t} + A_{\psi^2}(t,T)),$$

where $B_{\psi^2}(t,T)$ and $A_{\psi^2}(t,T)$ are the solutions to the following system of ODEs

$$\begin{aligned}
\frac{dB_{\psi^2}(t,T)}{dt} &= \rho^N + (K^Q)' B_{\psi^2}(t,T) - \frac{1}{2}\sum_{j=1}^{5}(\Sigma' B_{\psi^2}(t,T) B_{\psi^2}(t,T)'\Sigma)_{j,j}(\delta^j)', \quad B_{\psi^2}(T,T) = \overline{B},\\
\frac{dA_{\psi^2}(t,T)}{dt} &= -B_{\psi^2}(t,T)' K^Q \theta^Q - \frac{1}{2}\sum_{j=1}^{5}(\Sigma' B_{\psi^2}(t,T) B_{\psi^2}(t,T)'\Sigma)_{j,j}\gamma^j, \quad A_{\psi^2}(T,T) = 0.
\end{aligned}$$

This system can also be solved analytically and the solution is provided in the following proposition.

Proposition 2:

Let the state variables be given by $Z_{t,T} = (L_t^N, S_t, C_t, L_t^R, Y_{t,T})$, and let the nominal instantaneous risk-free rate be given by

$$r_t^N = (\rho^N)' X_t,$$

then

$$\psi^2(\overline{B}, t, T) = \exp(B^1_{\psi^2}(t,T) L_t^N + B^2_{\psi^2}(t,T) S_t + B^3_{\psi^2}(t,T) C_t + B^4_{\psi^2}(t,T) L_t^R + B^5_{\psi^2}(t,T) Y_{t,t} + A_{\psi^2}(t,T)),$$

where[38]

$$\begin{aligned}
B^1_{\psi^2}(t,T) &= \frac{-2\rho_1[e^{\phi^N_{\psi^2}(T-t)} - 1] + \overline{B}^1(\phi^N_{\psi^2} - \kappa^Q_{L^N})e^{\phi^N_{\psi^2}(T-t)} + \overline{B}^1(\phi^N_{\psi^1} + \kappa^Q_{L^N})}{2\phi^N_{\psi^2} + (\phi^N_{\psi^2} + \kappa^Q_{L^N} - \overline{B}^1\sigma^2_{11})[e^{\phi^N_{\psi^2}(T-t)} - 1]},\\
B^2_{\psi^2}(t,T) &= e^{-\lambda(T-t)}\overline{B}^2 - [1 - (1-\alpha^R)\overline{B}^5]\frac{1 - e^{-\lambda(T-t)}}{\lambda},\\
B^3_{\psi^2}(t,T) &= e^{-\lambda(T-t)}\overline{B}^3 + \lambda(T-t)e^{-\lambda(T-t)}\overline{B}^2 + [1 - (1-\alpha^R)\overline{B}^5]\Big\{(T-t)e^{-\lambda(T-t)} - \frac{1 - e^{-\lambda(T-t)}}{\lambda}\Big\},\\
B^4_{\psi^2}(t,T) &= \frac{-2\rho_4[e^{\phi^R_{\psi^2}(T-t)} - 1] + \overline{B}^4(\phi^R_{\psi^2} - \kappa^Q_{L^R})e^{\phi^R_{\psi^2}(T-t)} + \overline{B}^4(\phi^R_{\psi^2} + \kappa^Q_{L^R})}{2\phi^R_{\psi^2} + (\phi^R_{\psi^2} + \kappa^Q_{L^R} - \overline{B}^4\sigma^2_{44})[e^{\phi^R_{\psi^2}(T-t)} - 1]},\\
B^5_{\psi^2}(t,T) &= \overline{B}^5,
\end{aligned}$$

[38] The calculations leading to this result are available upon request.

and

$$
\begin{aligned}
A_{\psi^2}(t,T) \quad = \quad & \frac{2\kappa_{L^N}^Q \theta_{L^N}^Q}{\sigma_{11}^2} \ln\Bigg[\frac{2\phi_{\psi^2}^N e^{\frac{1}{2}(\phi_{\psi^2}^N+\kappa_{L^N}^Q)(T-t)}}{2\phi_{\psi^2}^N + (\phi_{\psi^2}^N + \kappa_{L^N}^Q - \overline{B}^1\sigma_{11}^2)[e^{\phi_{\psi^2}^N(T-t)} - 1]}\Bigg] \\
& +\sigma_{22}^2[1-(1-\alpha^R)\overline{B}^5 + \lambda\overline{B}^2]^2\frac{1-e^{-2\lambda(T-t)}}{4\lambda^3} + \frac{\sigma_{22}^2}{2}\frac{[1-(1-\alpha^R)\overline{B}^5]^2}{\lambda^2}(T-t) \\
& -\sigma_{22}^2[1-(1-\alpha^R)\overline{B}^5 + \lambda\overline{B}^2][1-(1-\alpha^R)\overline{B}^5]\frac{1-e^{-\lambda(T-t)}}{\lambda^3} \\
& +\sigma_{33}^2[1-(1-\alpha^R)\overline{B}^5 + \lambda\overline{B}^3]^2\frac{1-e^{-2\lambda(T-t)}}{4\lambda^3} + \frac{\sigma_{33}^2}{2}\frac{[1-(1-\alpha^R)\overline{B}^5]^2}{\lambda^2}(T-t) \\
& +\frac{\sigma_{33}^2}{2}[1-(1-\alpha^R)\overline{B}^5 + \lambda\overline{B}^2]^2\Big[-\frac{1}{2\lambda}(T-t)^2e^{-2\lambda(T-t)} - \frac{1}{2\lambda^2}(T-t)e^{-2\lambda(T-t)} + \frac{1-e^{-2\lambda(t-t)}}{4\lambda^3}\Big] \\
& -\sigma_{33}^2[1-(1-\alpha^R)\overline{B}^5 + \lambda\overline{B}^3][1-(1-\alpha^R)\overline{B}^5]\frac{1-e^{-\lambda(T-t)}}{\lambda^3} \\
& +\sigma_{33}^2\frac{[1-(1-\alpha^R)\overline{B}^5 + \lambda\overline{B}^3][1-(1-\alpha^R)\overline{B}^5 + \lambda\overline{B}^2]}{\lambda}\Big[-\frac{1}{2\lambda}(T-t)e^{-2\lambda(T-t)} + \frac{1-e^{-2\lambda(T-t)}}{4\lambda^2}\Big] \\
& -\sigma_{33}^2\frac{[1-(1-\alpha^R)\overline{B}^5][1-(1-\alpha^R)\overline{B}^5 + \lambda\overline{B}^2]}{\lambda}\Big[-\frac{1}{\lambda}(T-t)e^{-\lambda(T-t)} + \frac{1-e^{-\lambda(T-t)}}{\lambda^2}\Big] \\
& +\frac{2\kappa_{L^R}^Q \theta_{L^R}^Q}{\sigma_{44}^2} \ln\Bigg[\frac{2\phi_{\psi^2}^R e^{\frac{1}{2}(\phi_{\psi^2}^R+\kappa_{L^R}^Q)(T-t)}}{2\phi_{\psi^2}^R + (\phi_{\psi^2}^R + \kappa_{L^R}^Q - \overline{B}^4\sigma_{44}^2)[e^{\phi_{\psi^2}^R(T-t)} - 1]}\Bigg]
\end{aligned}
$$

with

$$
\phi_{\psi^2}^N = \sqrt{(\kappa_{L^N}^Q)^2 + 2\rho_1\sigma_{11}^2}, \quad \rho_1 = 1 - \overline{B}^5, \quad \phi_{\psi^2}^R = \sqrt{(\kappa_{L^R}^Q)^2 + 2\rho_4\sigma_{44}^2}, \quad \text{and} \quad \rho_4 = \overline{B}^5.
$$

With these results at our disposal, we can turn our attention to the pricing of the deflation protection option in the TIPS contract. From Duffie, Pan, and Singleton (2000) it follows that

$$
\begin{aligned}
E_t^Q\Big[e^{-\int_t^T r_s^R ds}e^{\overline{B}'Z_{t,T}}\mathbf{1}_{\{b'Z_{t,T}\leq z\}}\Big] \quad &= \quad \frac{\psi^1(\overline{B},t,T)}{2} - \frac{1}{\pi}\int_0^\infty \frac{Im\{e^{-ivz}\psi^1(\overline{B}+ivb,t,T)\}}{v}dv, \\
E_t^Q\Big[e^{-\int_t^T r_s^N ds}e^{\overline{B}'Z_{t,T}}\mathbf{1}_{\{b'Z_{t,T}\leq z\}}\Big] \quad &= \quad \frac{\psi^2(\overline{B},t,T)}{2} - \frac{1}{\pi}\int_0^\infty \frac{Im\{e^{-ivz}\psi^2(\overline{B}+ivb,t,T)\}}{v}dv.
\end{aligned}
$$

Since we interested in the condition

$$
Y_{t,T} = \int_t^T (r_s^N - r_s^R)ds \leq \ln(1+q),
$$

the expectations above should be evaluated at $b = (0,0,0,0,1)$, $z = \ln(1+q)$, and $\overline{B} = (0,0,0,0,0)$.

A similar approach can be used to calculate the NPV of the TIPS deflation protection option within the CV model (see Christensen et al. 2012 for details).

The functions $\frac{Im\{e^{-ivz}\psi^1(\overline{B}+ivb,t,T)\}}{v}$ and $\frac{Im\{e^{-ivz}\psi^2(\overline{B}+ivb,t,T)\}}{v}$ that need to be integrated in order to calculate the NPV of the TIPS deflation protection option have already converged to zero for values of v above 500, so we approximate the infinite integral in the pricing formulas by capping v at 1000 to err on the side of conservatism and use a step size of $\Delta v = 0.01$ in the numerical approximation, which is sufficient since the functions are clearly smooth.

C). Deflation Probabilities Within the SV Model

Christensen et al. (2012) use the CV model to generate deflation probabilities at various horizons appropriate for macroeconomic and monetary policy purposes. Similarly, the SV model can be used to calculate deflation probabilities, although additional steps are necessary. The change in the market-implied price index for the period from t until $t+\tau$ is given by

$$\frac{\Pi_{t+\tau}}{\Pi_t} = e^{\int_t^{t+\tau}(r_s^N - r_s^R)ds}.$$

We want to calculate the probability of the event that the change in the price index is below a certain critical level q. By implication, we are interested in the states of the world where

$$\frac{\Pi_{t+\tau}}{\Pi_t} \leq 1+q,$$

or, equivalently,

$$\int_t^{t+\tau}(r_s^N - r_s^R)ds \leq \ln(1+q).$$

Since the nominal and real instantaneous short rates are given by

$$\begin{aligned} r_t^N &= L_t^N + S_t, \\ r_t^R &= L_t^R + \alpha^R S_t, \end{aligned}$$

we are interested in the distributional properties of the following process

$$Y_{0,t} = \int_0^t (r_s^N - r_s^R)ds = \int_0^t (L_s^N + S_s - L_s^R - \alpha^R S_s)ds \quad \Rightarrow \quad dY_{0,t} = (L_t^N + (1-\alpha^R)S_t - L_t^R)dt.$$

In general, the P-dynamics of the state variables X_t are given by

$$dX_t = K^P(\theta^P - X_t)dt + \Sigma D(X_t)dW_t^P.$$

Adding the Y_t-process to this system, leaves us with a five-factor SDE of the following form

$$\begin{pmatrix} dL_t^N \\ dS_t \\ dC_t \\ dL_t^R \\ dY_{0,t} \end{pmatrix} = \begin{pmatrix} \kappa_{11}^P & 0 & 0 & \kappa_{14}^P & 0 \\ \kappa_{21}^P & \kappa_{22}^P & \kappa_{23}^P & \kappa_{24}^P & 0 \\ \kappa_{31}^P & \kappa_{32}^P & \kappa_{33}^P & \kappa_{34}^P & 0 \\ \kappa_{41}^P & 0 & 0 & \kappa_{44}^P & 0 \\ 0 & 0 & 0 & 0 & 0 \end{pmatrix} \begin{pmatrix} \theta_1^P \\ \theta_2^P \\ \theta_3^P \\ \theta_4^P \\ 0 \end{pmatrix} dt - \begin{pmatrix} \kappa_{11}^P & 0 & 0 & \kappa_{14}^P & 0 \\ \kappa_{21}^P & \kappa_{22}^P & \kappa_{23}^P & \kappa_{24}^P & 0 \\ \kappa_{31}^P & \kappa_{32}^P & \kappa_{33}^P & \kappa_{34}^P & 0 \\ \kappa_{41}^P & 0 & 0 & \kappa_{44}^P & 0 \\ -1 & -(1-\alpha^R) & 0 & 1 & 0 \end{pmatrix} \begin{pmatrix} L_t^N \\ S_t \\ C_t \\ L_t^R \\ Y_{0,t} \end{pmatrix} dt$$

$$+ \begin{pmatrix} \sigma_{11} & 0 & 0 & 0 & 0 \\ 0 & \sigma_{22} & 0 & 0 & 0 \\ 0 & 0 & \sigma_{33} & 0 & 0 \\ 0 & 0 & 0 & \sigma_{44} & 0 \\ 0 & 0 & 0 & 0 & 0 \end{pmatrix} \begin{pmatrix} \sqrt{L_t^N} & 0 & 0 & 0 & 0 \\ 0 & \sqrt{1} & 0 & 0 & 0 \\ 0 & 0 & \sqrt{1} & 0 & 0 \\ 0 & 0 & 0 & \sqrt{L_t^R} & 0 \\ 0 & 0 & 0 & 0 & 0 \end{pmatrix} \begin{pmatrix} dW_t^{L^N,P} \\ dW_t^{S,P} \\ dW_t^{C,P} \\ dW_t^{L^R,P} \\ dW_t^{Y,P} \end{pmatrix},$$

where $Z_{0,t} = (L_t^N, S_t, C_t, L_t^R, Y_{0,t})$ represents the augmented state vector.

This is a system of non-Gaussian state variables. As a consequence, we cannot use the approach detailed in Christensen et al. (2012). Instead, we use the Fourier transform analysis described in full generality for affine models in Duffie, Pan, and Singleton (2000). They provide a formula for calculating contingent expectations of the form

$$G_{\overline{B},\overline{b}}(y; Z_{t,t}, t, T) = E^P\Big[e^{-\int_t^T \rho_\psi' Z_{s,T}ds} e^{\overline{B}' Z_{t,T}} \mathbf{1}_{\{\overline{b} Z_{t,T} \leq y\}} \Big| \mathcal{F}_t\Big].$$

If we define

$$\psi(\overline{B}; Z_{t,t}, t, T) = E^P\Big[e^{-\int_t^T \rho_\psi' Z_{s,T}ds} e^{\overline{B}' Z_{t,T}}\Big] = e^{B_\psi(t,T)' Z_{t,t} + A_\psi(t,T)},$$

where $B_\psi(t,T)$ and $A_\psi(t,T)$ are solutions to a system of ODEs similar to the one outlined in Equations (19) and (20),[39] then Duffie, Pan, and Singleton (2000) show that

$$G_{\overline{B},\overline{b}}(y; Z_{t,t}, t, T) = \frac{\psi(\overline{B}; Z_{t,t}, t, T)}{2} - \frac{1}{\pi}\int_0^\infty \frac{\text{Im}[e^{-ivy}\psi(\overline{B} + iv\overline{b}; Z_{t,t}, t, T)]}{v} dv.$$

Here, we are interested in the cumulative probability function of $Y_{t,T}$ conditional on $Z_{t,t}$, that is, we are interested in the function $E^P[\mathbf{1}_{\{Y_{t,T} \leq y\}} | \mathcal{F}_t]$. From the result above it follows that we get the desired probability function if we fix

$$\overline{B} = 0, \quad \overline{b} = \begin{pmatrix} 0 \\ 0 \\ 0 \\ 0 \\ 1 \end{pmatrix}, \quad \rho_\psi = 0, \quad \text{and} \quad y = \ln(1+q).$$

Priced Deflation Probabilities Within the SV Model

The actual probability of deflation calculated above is determined by the estimated factor dynamics under the P-measure. Thus, it reflects the actual time series dynamics of the state variables. The priced probability of deflation, on the other hand, reflects the implicit probability of deflation needed to match the observed bond prices. Due to risk premia that reflect bond investor risk aversion, this measure can be different from the actual deflation probability. To calculate the priced probability of deflation, we replace the P-dynamics above with the Q-dynamics.

[39] Note, however, that the solutions differ from the formulas in Appendix B as we are now working under the P-measure. Thus, we rely on numerical approximations based on a fourth order Runge-Kutta method.

References

Adrian, Tobias and Hao Wu, 2010, "The Term Structure of Inflation Expectations," Federal Reserve Bank of New York Staff Reports #362.

Andersen, Torben G. and Luca Benzoni, 2010, "Do Bonds Span Volatility Risk in the U.S. Treasury Market? A Specification Test for Affine Term Structure Models," *Journal of Finance*, Vol. 65, No. 2, 603-653.

Campbell, John Y., Robert J. Shiller, and Luis M. Viceira, 2009, "Understanding Inflation-Indexed Bond Markets," *Brookings Papers on Economic Activity*, Spring, 79-120.

Cheridito, Patrick, Damir Filipović, and Robert L. Kimmel, 2007, "Market Price of Risk Specifications for Affine Models: Theory and Evidence," *Journal of Financial Economics*, Vol. 83, No. 1, 123-170.

Chernov, Mikhail and Philippe Mueller, 2012, "The Term Structure of Inflation Expectations," *Journal of Financial Economics*, Vol. 106, No. 2, 367-394.

Christensen, Jens H. E., Francis X. Diebold, and Glenn D. Rudebusch, 2011, "The Affine Arbitrage-Free Class of Nelson-Siegel Term Structure Models," *Journal of Econometrics*, Vol. 164, No. 1, 4-20.

Christensen, Jens H. E. and James M. Gillan, 2012, "Could the U.S. Treasury Benefit from Issuing More TIPS?," Working Paper 2011-16, Federal Reserve Bank of San Francisco.

Christensen, Jens H. E. and James M. Gillan, 2014, "Does Quantitative Easing Affect Market Liquidity?," Working Paper 2013-26, Federal Reserve Bank of San Francisco.

Christensen, Jens H. E., Jose A. Lopez, and Glenn D. Rudebusch, 2010, "Inflation Expectations and Risk Premiums in an Arbitrage-Free Model of Nominal and Real Bond Yields," *Journal of Money, Credit and Banking*, Supplement to Vol. 42, No. 6, 143-178.

Christensen, Jens H. E., Jose A. Lopez, and Glenn D. Rudebusch, 2012, "Extracting Deflation Probability Forecasts from Treasury Yields," *International Journal of Central Banking*, Vol. 8, No. 4, 21-60.

Christensen, Jens H. E., Jose A. Lopez, and Glenn D. Rudebusch, 2014a, "Can Spanned Term Structure Factors Drive Stochastic Yield Volatility?," Working Paper 2014-03, Federal Reserve Bank of San Francisco.

Christensen, Jens H. E., Jose A. Lopez, and Glenn D. Rudebusch, 2014b, "Do Central Bank Liquidity Facilities Affect Interbank Lending Rates?," *Journal of Business and Economic Statistics*, Vol. 32, No. 1, 136-151.

Christensen, Jens H. E. and Glenn D. Rudebusch, 2014, "Estimating Shadow-Rate Term Structure Models with Near-Zero Yields," *Journal of Financial Econometrics*, forthcoming.

Dai, Qiang and Kenneth J. Singleton, 2000, "Specification Analysis of Affine Term Structure Models," *Journal of Finance*, Vol. 55, No. 5, 1943-1978.

D'Amico, Stefania, Don H. Kim, and Min Wei, 2014, "Tips from TIPS: the Informational Content of Treasury Inflation-Protected Security Prices," Finance and Economics Discussion Series Working Paper 2014-24, Board of Governors of the Federal Reserve System.

Driessen, Joost, 2005, "Is Default Event Risk Priced in Corporate Bonds?," *Review of Financial Studies*, Vol. 18, No. 1, 165-195.

Duffee, Gregory R., 1999, "Estimating the Price of Default Risk," *Review of Financial Studies*, Vol. 12, No. 1, 197-226.

Duffee, Gregory R., 2002, "Term Premia and Interest Rate Forecasts in Affine Models," *Journal of Finance*, Vol. 57, No. 1, 405-443.

Duffie, Darrell, Jun Pan, and Kenneth Singleton, 2000, "Transform Analysis and Asset Pricing for Affine Jump Diffusions," *Econometrica*, Vol. 68, No. 6, 1343-1376.

Feldhütter, Peter and David Lando, 2008, "Decomposing Swap Spreads," *Journal of Financial Economics*, Vol. 88, No. 2, 375-405.

Fisher, Mark and Christian Gilles, 1996, "Term Premia in Exponential-Affine Models of the Term Structure," Manuscript, Board of Governors of the Federal Reserve System.

Fleckenstein, Mathias, Francis A. Longstaff, and Hanno Lustig, 2012, "The TIPS-Treasury Bond Puzzle," *Journal of Finance*, forthcoming.

Fleckenstein, Mathias, Francis A. Longstaff, and Hanno Lustig, 2013, "Deflation Risk," Manuscript, University of California at Los Angeles.

Grishchenko, Olesya V., Joel Vanden, and Jianing Zhang, 2013, "The Informational Content of the Embedded Deflation Option in TIPS," Finance and Economics Discussion Series Working Paper 2013-24, Board of Governors of the Federal Reserve System.

Gürkaynak, Refet S., Brian Sack, and Jonathan H. Wright, 2007, "The U.S. Treasury Yield Curve: 1961 to the Present," *Journal of Monetary Economics*, Vol. 54, No. 8, 2291-2304.

Gürkaynak, Refet S., Brian Sack, and Jonathan H. Wright, 2010, "The TIPS Yield Curve and Inflation Compensation," *American Economic Journal: Macroeconomics*, Vol. 2, No. 1, 70-92.

Harvey, A.C., 1989, *Forecasting, structural time series models and the Kalman filter,* Cambridge: Cambridge University Press.

Haubrich, Joseph G., George Pennacchi, and Peter Ritchken, 2012, "Inflation Expectations, Real Rates, and Risk Premia: Evidence from Inflation Swaps," *Review of Financial Studies*, Vol. 25, No. 5, 1588-1629.

Hu, Grace Xing, Jun Pan, and Jiang Wang, 2013, "Noise as Information for Illiquidity," *Journal of Finance*, Vol. 68, No. 6, 2341-2382.

Joslin, Scott, Kenneth Singleton, and Haoxiang Zhu, 2011, "A New Perspective on Gaussian Dynamic Term Structure Models," *Review of Financial Studies*, Vol. 24, No. 3, 926-970.

Kitsul, Yuriy and Jonathan H. Wright, 2013, "The Economics of Options-Implied Inflation Probability Density Functions," *Journal of Financial Economics*, Vol. 110, No. 3, 503-752.

Merton, Robert C., 1974, "On the Pricing of Corporate Debt: The Risk Structure of Interest Rates," *Journal of Finance*, Vol. 29, No. 2, 449-470.

Nelson, Charles R. and Andrew F. Siegel, 1987, "Parsimonious Modeling of Yield Curves," *Journal of Business*, Vol. 60, No. 4, 473-489.

Pflueger, Carolin E. and Luis M. Viceira, 2013, "Return Predictability in the Treasury Market: Real Rates, Inflation, and Liquidity," Manuscript, Harvard Business School.

Svensson, Lars E. O., 1995, "Estimating Forward Interest Rates with the Extended Nelson-Siegel Method," *Quarterly Review*, No. 3, Sveriges Riksbank, 13-26.

Swanson, Eric T. and John C. Williams, 2014, "Measuring the Effect of the Zero Lower Bound on Medium- and Longer-Term Interest Rates," *American Economic Review*, forthcoming.

Wright, Jonathan H., 2009, "Comment on Understanding Inflation-Indexed Bond Markets," *Brookings Papers on Economic Activity*, Spring, 126-138.